Inorganic Chemistry

Article

pubs.acs.org/IC

Copper(II) and Gallium(III) Complexes of *trans*-Bis(2-hydroxybenzyl) Cyclen Derivatives: Absence of a Cross-Bridge Proves Surprisingly More Favorable

Catarina V. Esteves, Joana Madureira, Luís M. P. Lima, Pedro Mateus, Isabel Bento, and Rita Delgado*

Instituto de Tecnologia Química e Biológica, Universidade Nova de Lisboa, Av. da República 2780−157 Oeiras, Portugal

Supporting Information

ABSTRACT: Two cyclen (1,4,7,10-tetraazacyclododecane) derivatives bearing *trans*-bis(2-hydroxybenzyl) arms, the 1,7-(2-hydroxybenzyl)-1,4,7,10-tetraazacyclododecane (H_2do2ph) and its cross-bridged counterpart (H_2cb-do2ph), have been synthesized, aiming toward the possible use of their copper(II) and gallium(III) complexes in nuclear medicine. The protonation of both compounds was studied in aqueous solution as well as their complexes with Cu^{2+} and Ga^{3+} cations. The complexes of both ligands with Ca^{2+} and Zn^{2+} metal ions were also studied due to the abundance of these cations in biological media. In mild conditions the complexes of Ca^{2+} and Ga^{3+} with H_2cb-do2ph did not form. The behavior of the two ligands and their complexes was compared by the values of the equilibrium constants, the data of varied spectroscopic techniques, the values of redox potentials of their copper(II) complexes, and the resistance of the complexes to acid dissociation. It was expected that, as found for related pairs of cyclen and cyclam (1,4,8,11-tetraazacyclotetradecane) derivatives, the cross-bridged macrocyclic derivative could be an excellent ligand for the complexation of copper(II). Additionally, the *N*-2-hydroxybenzyl groups were chosen due to their known ability to coordinate the gallium(III) cation. Due to the small size of the latter cation and its particular propensity to form hexacoordinate complexes, it was also expected that there would be a good ability of both ligands for the uptake of Ga^{3+}. Surprisingly, the results revealed that the cyclen derivative H_2do2ph is the best ligand for the coordination of Cu^{2+} and Ga^{3+} cations, not only from their thermodynamic stability as expected but also from their kinetic inertness, when compared with its cross-bridged counterpart.

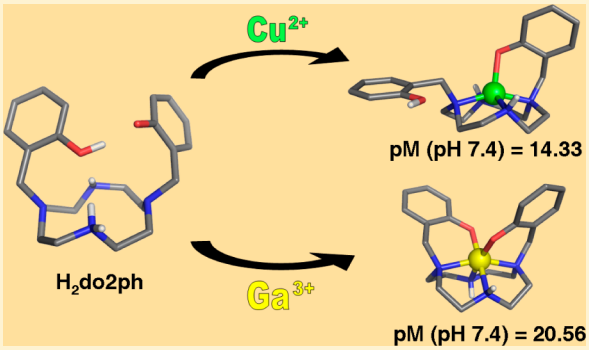

INTRODUCTION

The search for ligands capable of forming metal complexes with high thermodynamic stability, fast complexation kinetics, and high inertness toward dissociation for safe use in medicinal applications continues to be a challenging research field.[1−4] Metal complexes of noncyclic ligands usually form rapidly but are not very inert systems toward dissociation, while complexes of macrocyclic ligands are more kinetically inert and have larger thermodynamic stability but display slower rates of complexation.[1,3−5] On the other hand, macrobicyclic ligands, namely the cross-bridged ones derived from tetraazamacrocycles, form complexes even slower but that are much more inert toward dissociation,[6−10] and most of them are selective for copper(II) metal ions.[10−12] Generally, the more preorganized the ligand is, the slower the formation and dissociation of its metal complexes is.

Therefore, to avoid premature *in vivo* demetalation of the complexes or metal transchelation to proteins, cyclic ligands (macrocycles or macrobicycles) have been preferred, especially those that are preorganized, in which the size of the cavity and the number and the type of donor atoms match the size, the geometrical, and the stereochemical requirements of the metal ion. These features are particularly important for bifunctional chelates (BFC) used in noninvasive imaging techniques such as positron emission tomography (PET) and single photon emission computed tomography (SPECT), or in radioimmunotherapy (RIT) of tumors. The BFC is composed of a metallic radioisotope complex to which a targeting biomolecule, capable of binding to specific receptors overexpressed in certain tumors or organs in the body, is covalently bound to a suitable point of the ligand framework.[3,13,14] This is especially important when short-lived radionuclides are used, as is the case of the most used positron emitters ^{68}Ga ($t_{1/2}$ = 1.13 h) and ^{64}Cu($t_{1/2}$ = 12.8 h).[3,4,15,16] Other isotopes are also suitable for nuclear imaging, such as ^{67}Ga ($t_{1/2}$ = 78.3 h; γ-emitter) used in SPECT and therapy, and ^{66}Ga ($t_{1/2}$ = 9.4 h; β^+-emitter).[1,3,16,17] In addition to ^{64}Cu, other interesting copper isotopes are ^{62}Cu ($t_{1/2}$ = 0.16 h, β^+-emitter) that is generator produced, and ^{67}Cu ($t_{1/2}$ = 62.01 h, β^--emitting) that is only produced at high-energy accelerators.[2,3,18] Therapeutic radiopharmaceuticals for RIT deliver cytotoxic nonpenetrating radiation (Auger electrons and β^- or α particles) doses to diseased sites, resulting in the death of the cancer cells. Therapeutic nuclear medicine is

Received: December 27, 2013
Published: April 22, 2014

   dx.doi.org/10.1021/ic403156h | Inorg. Chem. 2014, 53, 4371−4386

less advanced than imaging techniques but has enormous potential if the radionuclide is accurately targeted.[18]

The aim of the present work is to compare the behavior of two novel cyclen derivatives with *trans*-bis(2-hydroxybenzyl) pendant arms and different degrees of preorganization, the H_2do2ph and its cross-bridged counterpart (H_2cb-do2ph), see Chart 1. Until very recently, cyclen derivatives with phenolic

Chart 1. Structures of Compounds Discussed in This Work

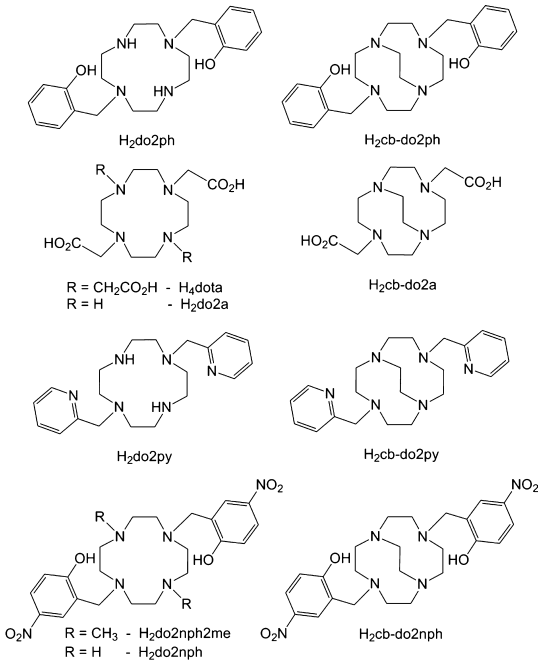

pendant arms had not been used for complexation of copper(II), except in the case of H_2do2nph2me.[19] Last year we reported the study of two cyclen derivatives H_2do2nph and H_2cb-do2nph containing two 2-methyl-4-nitrophenol pendant arms, where it was found that they present a good chelation ability for copper(II), especially the cross-bridged one that yielded a distorted octahedral coordination mode.[20] However, the rather low solubility of the ligands and their complexes in aqueous media limited the range of studies that could be performed. We were nonetheless convinced of the promise of such ligand structure for efficiently binding copper(II) and predictably also gallium(III).

Therefore, in this work 2-hydroxybenzyl arms replaced the 2-methyl-4-nitrophenol ones used in the previous report, resulting in compounds with excellent water solubility. It was expected that the cross-bridged macrocyclic derivative could be an excellent ligand for the complexation of copper(II) and also gallium(III), due to its rigid backbone and the appropriate size of the cavity for the inclusion of these cations. The phenolic pendant arms were selected due to their known ability to coordinate the gallium(III) and also copper(II) cations. The properties of the copper(II) and gallium(III) complexes were thoroughly studied, including the thermodynamic, kinetic, and electrochemical stabilities of the complexes in aqueous solution, and their structural properties in solution and in the solid state. The behavior of the pair of ligands now studied will be compared with the very few available data of other pairs of cyclen derivatives bearing different pendant arms, see Chart 1.[10,11,20] These studies also allowed us to evaluate if the compounds are adequate from the chemical point of view for applications in nuclear medicine.

RESULTS AND DISCUSSION

Synthesis of the Ligands. The compound H_2cb-do2ph was prepared by slight adaptation of the method used to synthesize its previously reported methylnitrophenolic analogue,[20] as illustrated in Scheme 1. Bisquaternarization of cyclen-glyoxal

Scheme 1. Synthetic Procedures[a]

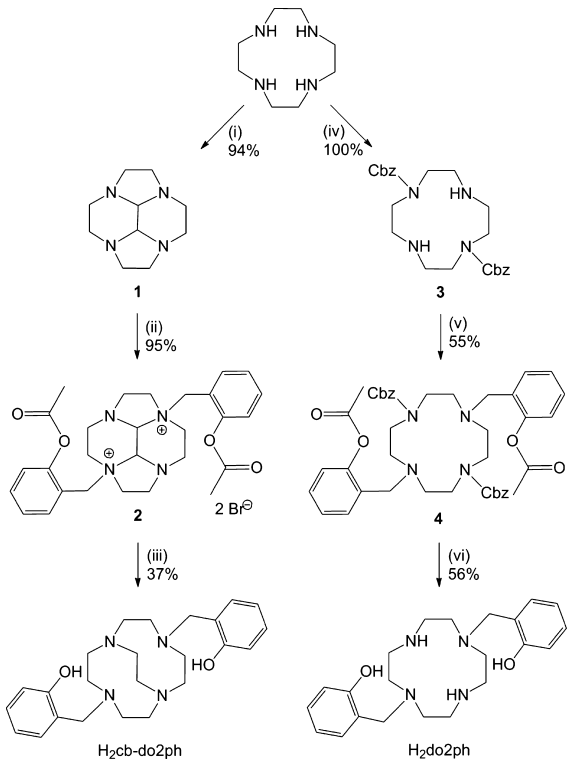

[a]Synthetic procedure used to obtain H_2do2ph and H_2cb-do2ph: (i) glyoxal trimer, MeOH, 0 °C, rt, 2.5 h; (ii) 2-(bromomethy1)phenyl acetate, MeCN, rt, 7 d; (iii) $NaBH_4$, EtOH/H_2O (9:1), rt, 24 h; 1 M KOH, 70 °C, 12 h; (iv) CbzCl, $CHCl_3$, 0 °C; (v) 2-(bromomethy1)-phenyl acetate, MeCN, 40 °C, 3 d and 60 °C, 4 d; (vi) 33% HBr, rt, 1 h; 0.1 M NaOH, rt, 12 h.

(**1**)[21] with 2 equiv of 2-(bromomethy1)phenyl acetate produced the cyclen-glyoxal *trans*-bis(2-methylphenyl acetate) diammonium bromide (**2**) in nearly quantitative yield. Sodium borohydride reduction in ethanol/water[22] followed by hydrolysis of the acetate groups in basic medium afforded the desired compound. Care must be taken not to expose the compound to highly acidic hydrochloric or nitric media due to the formation of intractable insoluble compounds, probably resulting from electrophilic aromatic substitution reactions.

Attempts to synthesize the compound H_2do2ph by deprotection of cyclen-glyoxal *trans*-bis(2-methylphenyl acetate) diammonium bromide (**2**) with hydrazine monohydrate,[23] hydroxylamine,[24] or NaOH[25] failed. Alternatively, the benzyloxycarbonyl (Cbz) *trans*-*N*-diprotected cyclen derivative **3**[26] (see Scheme 1) was dialkylated at the remaining *trans* positions with 2-(bromomethy1)phenyl acetate to yield compound **4**. The removal of the Cbz groups in acidic medium followed by basic hydrolysis of the acetate functions afforded the H_2do2ph compound in reasonable yield.

dx.doi.org/10.1021/ic403156h | Inorg. Chem. 2014, 53, 4371−4386

X-ray Diffraction Structures of H_2do2ph and Its Copper(II) and Gallium(III) Complexes. *Structure of H_2do2ph.* The asymmetric unit of the H_2do2ph compound, presented in Figure 1 with the labeling scheme adopted, shows

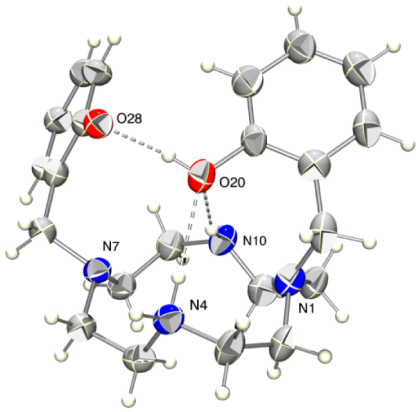

Figure 1. ORTEP view of H_2do2ph with the atomic labeling scheme and thermal ellipsoids drawn at the 50% probability level.

a secondary nitrogen atom (N4) and one phenolic oxygen atom (O20) protonated as revealed by the last difference Fourier maps calculated along the structure refinement. The cyclen ring exhibits the usual [3333] conformation[27] with all nitrogen atoms pointing to the same side of the macrocycle, with a distance between the *trans* tertiary amine nitrogen atoms of 4.360(7) Å, while the secondary ones are 4.013(7) Å apart (Table 1). The protonated phenolic oxygen atom lies 2.438 Å

Table 1. Intramolecular N···N and Selected N···O Distances (Å) on the Macrocyclic Backbone of H_2do2ph

N1···N4	2.858(7)
N1···N7	4.360(7)
N1···N10	2.926(8)
N4···N7	3.047(7)
N4···N10	4.013(7)
N7···N10	3.027(6)
N1···O20	2.942(6)
N4···O20	3.111(6)
N7···O20	3.591(6)
N10···O20	3.309(8)

above the mean plane defined by the four nitrogen atoms and receives two N−H···O hydrogen bonds from the secondary amines of the macrocycle, exhibiting N···O distances of 3.309(8) and 3.111(6) Å, see Table 2. In addition, this phenolic OH group establishes a strong hydrogen bond with the oxygen atom of the phenolate pendant arm, with an O···O distance of 2.553(5) Å and O−H···O angle of 168.4(3)°. A strong hydrogen bond between both phenolic arms was also observed in the structure of the related methylnitrophenolic

Table 2. Hydrogen Bond Dimensions of H_2do2ph

D−H···A*	H···A/Å	D···A/Å	D−H···A/deg
N4−H4b···O20	2.185(4)	3.111(6)	159.4(3)
N10−H10···O20	2.40(7)	3.309(8)	164(5)
O20−H20a···O28	1.743(3)	2.553(5)	168.4(3)

*D = N or O; A = O.

compound $(H_3$do2nph2me$)Br$[20] (see Chart 1 for the molecular representation of the compound); however, in this case the protonation state of the ligand is different.

Structure of [Cu(Hdo2ph)]ClO_4·H_2O. The asymmetric unit of the copper(II) complex of H_2do2ph is composed of a $[Cu(Hdo2ph)]^+$ cation, one ClO_4^- counterion, and a crystallization water molecule, giving rise to the molecular formula $[Cu(Hdo2ph)]ClO_4·H_2O$. Selected bond distances and angles in the coordination sphere of $[Cu(Hdo2ph)]^+$ were collected in Table 3. The copper center exhibits a distorted square

Table 3. Selected Bond Distances (Å) and Angles (deg) in the Coordination Spheres of the $[Cu(Hdo2ph)]^+$ and $[Ga(do2ph)]^+$ Cation Complexes

complex	$[Cu(Hdo2ph)]^+$	$[Ga(do2ph)]^+$
Bond Lengths/Å		
M−N1	2.038(4)	2.095(2)
M−N4	2.035(4)	2.091(2)
M−N7	2.031(4)	2.104(2)
M−N10	2.038(4)	2.116(2)
M−O20	2.101(4)	1.963(4)
M−O28		1.892(1)
Bong Angles/deg		
N1−M−N7	153.3(1)	157.33(7)
N4−M−N10	145.8(1)	94.90(7)
N1−M−N10	85.8(2)	80.86(7)
N4−M−N1	86.5(1)	84.34(7)
N7−M−N4	86.4(1)	83.57(7)
N7−M−N10	85.7(1)	81.15(7)
O20−M−N7	110.9(1)	105.69(6)
O20−M−N10	110.5(1)	172.87(7)
O20−M−N1	95.7(1)	92.01(7)
O20−M−N4	103.4(1)	84.03(6)
N4−M−N1		84.34(7)
N4−M−O28		174.15(7)
N1−M−O28		99.66(7)
N10−M−O28		89.97(7)
N7−M−O28		94.01(6)
O20−M−O28		91.54(6)

pyramidal coordination environment with the four nitrogen atoms of the cyclen ring defining the basal plane and an oxygen atom of one of the 2-methylphenol arms occupying the apical position (Figure 2). The copper atom is positioned above the N_4 coordination plane by 0.534 Å, pointing toward the apical

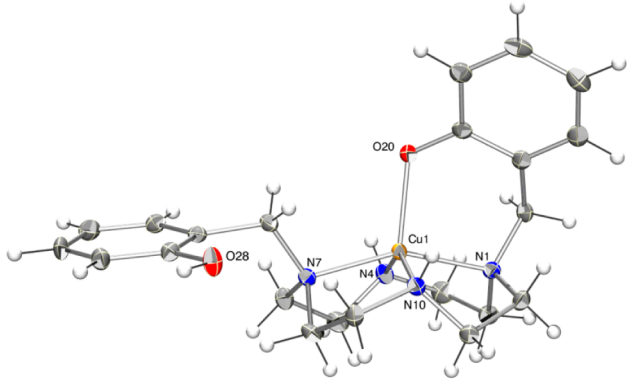

Figure 2. ORTEP view of $[Cu(Hdo2ph)]^+$ with the atomic labeling scheme and thermal ellipsoids drawn at the 50% probability level.

dx.doi.org/10.1021/ic403156h | Inorg. Chem. 2014, 53, 4371−4386

oxygen atom from the coordinated 2-methylphenol arm. The trigonal distortion calculated using the index structural parameter τ ($\tau = 0$ for a perfect square-pyramidal geometry and $\tau = 1$ for an ideal trigonal-bipyramidal geometry, as previously defined by Addison et al.)[28] assumes a value of 0.125 which is consistent with a distorted square pyramidal coordination sphere. The cyclen ring adopts the [3333] conformation already observed in the free ligand H_2do2ph, which suggests that only a small conformational rearrangement occurs upon coordination.

The structure of this complex is very similar to those of the related complexes $[Cu(Hdo2nph)]^+$,[20] and $[Cu(Hdo2nph2me)]^+$.[19] Indeed, the mean Cu−N and Cu−O distances of 2.036 and 2.101 Å, respectively, compare well with the mean Cu−N and Cu−O distances of 2.031 and 2.079 Å for $[Cu(Hdo2nph)]^+$,[20] and 2.046(14) and 2.095 Å for $[Cu(Hdo2nph2me)]^+$.[19]

Structure of [Ga(do2ph)]NO_3·2H_2O. The asymmetric unit of the gallium(III) complex of H_2do2ph is composed of the $[Ga(do2ph)]^+$ complex cation, one NO_3^- anion, and two crystallization water molecules, giving rise to the molecular formula $[Ga(do2ph)]NO_3·2H_2O$. The complex cation $[Ga(do2ph)]^+$ is shown in Figure 3 along with the relevant atomic notation

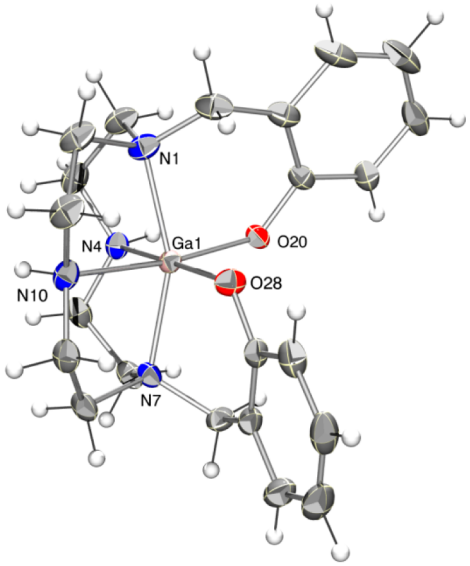

Figure 3. ORTEP view of $[Ga(do2ph)]^+$ complex cation with the atomic labeling scheme and thermal ellipsoids drawn at the 50% probability level.

adopted. The complex displays a *cis*-distorted octahedral geometry comprising the four nitrogen atoms of the macrocycle and two phenolic oxygen atoms. The N1 and N7 donors occupy the axial positions as the Ga−N1 and Ga−N7 bond lengths add up to the highest possible sum [4.199(2) Å] and the respective angle of 157.33(7)° gives a measure of the extent of distortion from a perfect octahedral geometry. The two secondary amine nitrogen atoms and the two phenolate oxygen atoms occupy the equatorial positions forming an almost perfect plane with a maximum mean plane deviation of 0.100 Å, with the Ga center positioned at 0.031 Å from this plane. The average Ga−N and Ga−O bond lengths (see Table 3) are within the expected range for complexes of amine phenol type ligands [d(Ga−N) = 2.090−2.183 Å and d(Ga−O) = 1.854−1.954 Å].[15]

The coordination mode of $[Ga(do2ph)]^+$ is similar to those found in the structures of all reported gallium(III) complexes of related dota-like ligands (cyclen derivatives with acetate pendant arms),[29−33] although some differences are noteworthy. In all cases two nitrogen atoms of the macrocycle occupy the apical positions, although in the $[Ga(do2ph)]^+$ complex the $d(Ga−N)_{ax}$ is slightly below the range found in the dota-like complexes (2.117−2.187 Å) and the $N_{ax}−Ga−N_{ax}$ angle is slightly above (156.3−157.1°). Interestingly, although in all *cis*-octahedral gallium(III) complexes of dota-like ligands the macrocyclic framework adopts a [2424] conformation with a type I arrangement (Bosnich nomenclature),[34] and having the coordinated carboxylate pendant arms bound to the equatorial macrocyclic nitrogen atoms, in $[Ga(do2ph)]^+$ the macrocycle displays the type II arrangement with the coordinated phenolate pendant arms attached on the axial nitrogen atoms. In this regard the structure reported here bears higher similarity to the $[Ga(cb\text{-}do2a)]^+$ one, due to the ethylenic cross-bridge displaying a [2424] conformation with a type V arrangement and coordinated carboxylate pendant arms attached to the axial instead of equatorial nitrogen atoms.[35]

Acid−Base Properties of the H_2do2ph and H_2cb-do2ph Compounds. The compounds H_2do2ph and H_2cb-do2ph have six basic centers consisting of the four amines and the two phenol functions. From potentiometric titrations in aqueous solution at 298.2 ± 0.1 K and ionic strength of 0.10 ± 0.01 M in KNO_3, five protonation constants of H_2do2ph and only three of H_2cb-do2ph could be accurately determined. The overall (β_i^H) and stepwise (K_i^H) protonation constants are compiled in Table 4, together with reported values for H_2do2a,[36] H_4dota,[37,38] do2py, and cb-do2py[11] for comparison.

Cross-bridged derivatives of tetraaza macrocycles are well-known for their strongly basic properties, where the first protonation constant usually assumes very large values and is frequently outside the possible scope of determination by potentiometric and sometimes even spectroscopic techniques,[10,11] as was also found for H_2cb-do2ph. A ^{1}H NMR titration of this compound in D_2O solution in the range of pD 3−15 was performed, but even in this solvent the final deprotonation step of the compound is barely starting at pD > 14. Thus, in order to allow for comparison of the stability constants of H_2cb-do2ph with H_2do2ph and literature compounds, a value of 15.0 (in log units) was postulated for the mentioned first protonation constant of H_2cb-do2ph. A ^{1}H NMR titration was also performed for H_2do2ph in the range pD 3−14. The two NMR titrations (Figures S1−S2 of Supporting Information) allowed for determination of protonation constants for both compounds (presented in Table 4 in square brackets), and in spite of the higher standard deviations arising from the experimental limitations, they are in very good agreement with the values determined by potentiometry.

The two compounds, H_2do2ph and H_2cb-do2ph, differ enormously in protonation constant values, the first constant being much larger and the fourth one much smaller for the cross-bridged macrocycle. These differences can be observed in Figure S3 of Supporting Information where the speciation diagrams of both compounds as a function of pH are represented. In Supporting Information Figure S3 (left) it can be seen that the maximum percentage of H_3do2ph$^+$ is formed at pH 9 and the total deprotonation of this compound is found at pH about 12.5, while for the cross-bridged derivative the maximum percentage of H_3cb-doph$^+$ species exists at pH 7, and at pH 14 only a very small amount of the cb-doph^{2-} species is

dx.doi.org/10.1021/ic403156h | Inorg. Chem. 2014, 53, 4371−4386

Table 4. Overall (β_i^H) and Stepwise (K_i^H) Protonation Constants, in log Units, of H_2do2ph and H_2cb-do2ph at 298.2 K in 0.10 M KNO_3 with Values for Some Related Compounds Also Included

equilibrium reaction[a]	H_2do2ph[b]	H_2cb-do2ph[b]	H_2do2a[c]	H_4dota[d]	do2py[e]	cb-do2py[e]
		log β_i^H				
$L + H^+ \rightleftarrows HL$	11.32(3)	15.0[f]	11.45	12.09	9.90	13.8
$L + 2\,H^+ \rightleftarrows H_2L$	22.48(2)	25.34(1)	20.99	21.85	18.30	19.11
$L + 3\,H^+ \rightleftarrows H_3L$	32.41(2)	34.95(1)	24.99	26.41	22.05	23.07
$L + 4\,H^+ \rightleftarrows H_4L$	39.97(2)	39.55(1)	27.35	30.50	24.55	25.53
$L + 5\,H^+ \rightleftarrows H_5L$	41.63(3)					
		log K_i^H				
$L + H^+ \rightleftarrows HL$	11.32 [11.36]	15.0[f]	11.45	12.09	9.90	13.8
$HL + H^+ \rightleftarrows H_2L$	11.16 [11.35]	10.34 [10.72]	9.54	9.76	8.40	5.31
$H_2L + H^+ \rightleftarrows H_3L$	9.93 [10.07]	9.61 [9.72]	4.00	4.56	3.75	3.96
$H_3L + H^+ \rightleftarrows H_4L$	7.56 [7.83]	4.60 [4.8]	2.36	4.09	2.50	2.46
$H_4L + H^+ \rightleftarrows H_5L$	1.66					

[a]L denotes the ligand in general; charges of the species are omitted for clarity. [b]This work; values in parentheses are standard deviations in the last significant figures, and in square brackets were included the values determined by ^{1}H NMR titrations. [c]T = 298.2 K, I = 0.10 M in NEt_4ClO_4.[36] [d]T = 298.2 K, I = 0.10 M in NMe_4NO_3.[37,38] [e]T = 298.2 K, I = 0.10 M in NMe_4NO_3.[11] [f]Value impossible to determine accurately, see text.

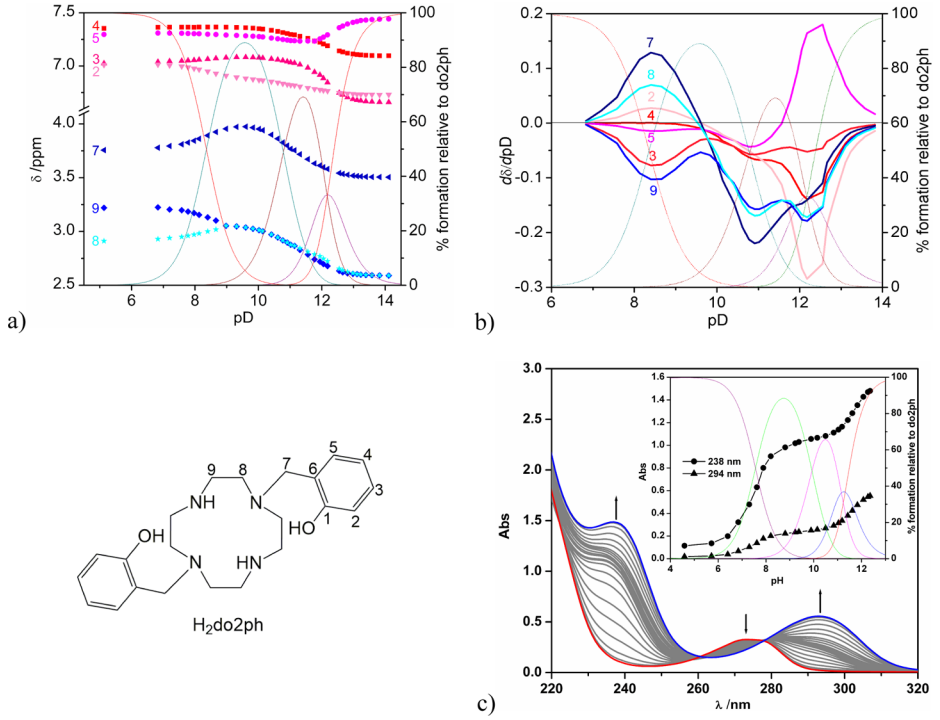

Figure 4. Spectral variations with pH of the compound H_2do2ph: (a) ^{1}H NMR experimental chemical shifts as a function of pD upon titration in D_2O with KOD at 298.2 K; (b) first derivative of the calculated chemical shifts; (c) UV spectra in aqueous solution at increasing pH values. Inset: values of the absorbance at 238 and 294 nm as a function of pH. The plots a), b), and the inset were drawn over the corresponding speciation diagram.

formed in solution. However, these results do not give information about the basic center that is protonated at a given pH. This information, which is crucial for the interpretation of the values, can be retrieved from the NMR titrations and, due to the presence of the phenolic arms, assisted by UV spectra in aqueous solutions in the range pH 2.8−12.4 (Figures S4−S5 of Supporting Information), as detailed below.

Actually, the acid−base behavior of H_2do2ph displays some particularities that are worthy of a deeper discussion. The first two log K_i^H values are rather similar (11.32 and 11.16), and according to the determined crystal structure (see above), it is expected that also in solution one of the protonation constants must be assigned to the protonation of a secondary amine and the other to the protonation of one phenolate group. Evidence that the same happens in solution is provided by the NMR spectra recorded in the pD range 11.6−14.0 which shows considerable shifts of the resonances corresponding to both cyclen and phenol protons (Figure 4a,b).

In addition, the decrease of intensity of the bands at 238 and 294 nm in the UV spectra, assigned to the $\pi-\pi^*$ transitions of phenolate, and concomitant increase of a band at 274 nm attributable to the phenol form clearly show the protonation of a phenolate group occurring at the pH 12.4−10.5 region (Figure 4c).

Although the available data does not allow unambiguous assignment of each protonation constant to the respective basic center, it is clear that the protonation of the first secondary amine occurs at the pH that is typical in cyclen derivatives while

dx.doi.org/10.1021/ic403156h | Inorg. Chem. 2014, 53, 4371−4386

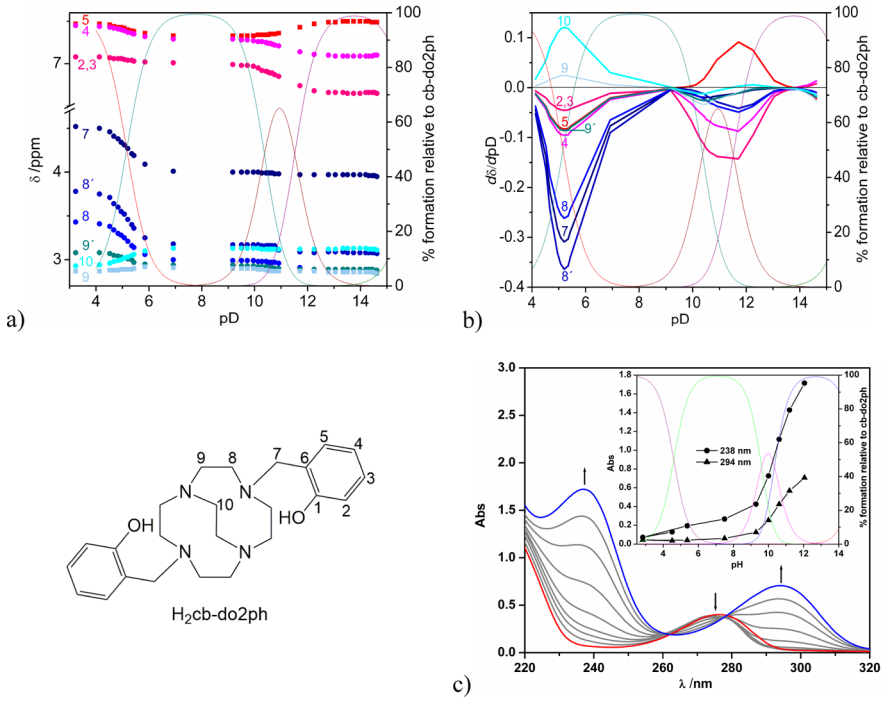

Figure 5. Spectral variations with pH of the cross-bridged compound, H_2cb-do2ph: (a) ^{1}H NMR experimental chemical shifts as a function of pD upon titration in D_2O with KOD at 298.2 K; (b) first derivative of the calculated chemical shifts; (c) UV spectra in aqueous solution at increasing pH values. Inset: values of the absorbance at 238 and 294 nm as a function of pH. The plots a), b) and the inset were drawn over the corresponding speciation diagram.

the basicity of the phenol pendant is very high when compared to the log K_i^H of phenol (9.79) or of 2-(aminomethyl)phenol (8.63).[39] This unusual fact may be explained by the formation of a strong hydrogen bond between the phenol pendant and the phenolate one (O−H···$^-$O), and additional hydrogen bonds between both secondary ring amines and the phenol (N−H···OH), as evidenced also in the crystal structure. The third log K_i^H is assigned to the other secondary amine as evidenced by the pronounced downfield shift of the resonances of cyclen protons 7, 8, and 9 as the pD drops from 11.6 to 9.6 and by the small shift observed for the phenol proton resonances in the same pD region (Figure 4a). The UV spectra show almost no changes in the bands at the pH 8.8−10.5 region (Figure 4c) which confirms that the remaining phenolate is not being protonated in this pH range. Below pH 8.8 the two UV bands at 238 and 294 nm disappear to give rise to a single band at 274 nm, providing unequivocal evidence for the protonation of the second phenolate arm. The log K_i^H value of 7.56 is quite lower than that of phenol or of 2-(aminomethyl)-phenol because this protonation causes disruption of the strong hydrogen bond between the phenol and phenolate pendant arms (O−H···$^-$O). Interestingly, the NMR spectra for pD < 9.6 showed only small shifts in the phenol proton resonances and larger shifts in the cyclen ones (Figure 4). These odd resonance shift variations may be explained by the disruption of the strong O−H···$^-$O hydrogen bond and concomitant movement of one of the phenols to a position away from the macrocyclic cavity, as observed in the crystal structure of the related H_4do2nph^{2+} compound. Simultaneous rearrangements of the macrocyclic backbone can also account for this behavior.

In contrast with H_2do2ph, the acid−base behavior of H_2cb-do2ph displays the features expected for a cross-bridged cyclen derivative with phenol pendant arms. The first protonation occurs on the amines at very high pH, with probable delocalization of the proton by strong hydrogen bonds with all amines, and it could not be fully observed. Both ^{1}H NMR and UV spectra (Figure 5) clearly show the three remaining protonation steps, with the two highest log K_i^H assigned to the consecutive protonations of both phenolate pendant arms without any noticeable hydrogen bonding effects, unlike for H_2do2ph. The lowest log K_i^H corresponds to the protonation of a second ring amine, and its significantly lower value is a consequence of the necessary disruption of the hydrogen bonding pattern involving all ring amines and the stretched cavity shape that are usual in cross-bridged tetraaza macrocycles.[10,11,19]

Stability Constants of Metal Complexes. The ability of H_2do2ph and H_2cb-do2ph to form complexes with Ca^{2+}, Cu^{2+}, Zn^{2+}, and Ga^{3+} cations was evaluated in aqueous solution, and their thermodynamic stability constants were determined in conditions similar to those used for the determination of protonation constants. The complexes of Zn^{2+} and Ca^{2+} cations were also studied due to its abundance in biological media. The obtained values were compiled in Table 5 together with those for the complexes of related ligands for comparison reasons.[11,33,36−38,40] The corresponding species distribution diagrams are shown in Figure 6 for the complexes of Cu^{2+} and Ga^{3+} with H_2do2ph, and in Figure 7 for the complex of copper(II) with H_2cb-do2ph (in Supporting Information Figures S6−S7 for the remaining complexes).

The complexation reactions of H_2do2ph are generally slow on the acidic pH range except with the Ca^{2+} cation. For Cu^{2+} it was necessary to perform a batch titration at the acidic pH range in order to complement the in-cell titrations. In the case of Ga^{3+}, the stability constants had to be determined by OH^- competition on the basis of the dissociation equilibrium of the complex at basic pH and formation of the $Ga(OH_4)^-$ species,[41,42] which could nonetheless be followed by in-cell

dx.doi.org/10.1021/ic403156h | Inorg. Chem. 2014, 53, 4371−4386

Table 5. Overall (β_{MH_iL}) and Stepwise (K_{MH_iL}) Stability Constants, in log Units, of Metal Complexes of H_2do2ph, H_2cb-do2ph, and Other Related Ligands at 298.2 K in 0.10 M KNO_3

equilibrium reaction[a]	H_2do2ph[b]	H_2cb-do2ph[b]	H_2do2a[c]	H_4dota	do2py[d]	cb-do2py[d]
			log β_{MH_iL}			
$Ca^{2+} + L + H^+ \rightleftarrows CaHL$	14.50(4)	*e*		20.77[f]		
$Ca^{2+} + L \rightleftarrows CaL$	5.07(1)	*e*		17.23[f]		
$Ca^{2+} + L \rightleftarrows CaLOH + H^+$	−6.57(1)	*e*				
$Cu^{2+} + L + 2H^+ \rightleftarrows CuH_2L$	37.81(2)					
$Cu^{2+} + L + H^+ \rightleftarrows CuHL$	32.34(3)	34.08(5)	24.1	26.03[f]	23.11	22.86
$Cu^{2+} + L \rightleftarrows CuL$	22.83(4)	25.06(4)	21.1	22.25[f]	20.3	19.03
$Cu^{2+} + L \rightleftarrows CuLOH + H^+$					13.0	
$Zn^{2+} + L + 2H^+ \rightleftarrows ZnH_2L$	33.19(9)					
$Zn^{2+} + L + H^+ \rightleftarrows ZnHL$	28.88(1)	27.48(1)	22.2	25.28[f]	20.73	
$Zn^{2+} + L \rightleftarrows ZnL$	19.33(2)	20.79(2)	18.2	21.10[f]	17.51	17.10
$Zn^{2+} + L \rightleftarrows ZnLOH + H^+$	7.57(3)	11.09(4)			10.67	
$Ga^{3+} + L + H^+ \rightleftarrows GaHL$	34.5(1)	35.19(2)		25.33[g]		
$Ga^{3+} + L \rightleftarrows GaL$	31.16(3)	31.82(1)		21.33;[g] 26.05[h]		
			log K_{MH_iL}			
$CaL + H^+ \rightleftarrows CaHL$	9.43			3.54[f]		
$Ca^{2+} + L \rightleftarrows CaL$	5.07			17.23[f]		
$CaLOH + H^+ \rightleftarrows CaL$	11.64					
$CuHL + H^+ \rightleftarrows CuH_2L$	5.47					
$CuL + H^+ \rightleftarrows CuHL$	9.51	9.02	3.0	3.78[f]	2.81	3.83
$Cu^{2+} + L \rightleftarrows CuL$	22.83	25.06	21.1	22.25[f]	20.3	19.03
$Cu^{2+} + L \rightleftarrows CuLOH + H^+$					7.3	
$ZnHL + H^+ \rightleftarrows ZnH_2L$	4.31					
$ZnL + H^+ \rightleftarrows ZnHL$	9.55	6.69	4.0	4.18[f]	3.22	
$Zn^{2+} + L \rightleftarrows ZnL$	19.33	20.79	18.2	21.10[f]	17.51	17.10
$ZnLOH + H^+ \rightleftarrows ZnL$	11.76	9.70			6.84	
$GaL + H^+ \rightleftarrows GaHL$	3.34	*e*		4.00;[g] 3.64[h]		
$Ga^{3+} + L \rightleftarrows GaL$	31.16	*e*		21.33;[g] 26.05[h]		

[a] L denotes the ligand; charges of the species are omitted for clarity. [b] This work; values in parentheses are standard deviations in the last significant figures. [c] T = 298.2 K, I = 0.1 M in NEt_4ClO_4.[36] [d] T = 298.2 K, I = 0.10 M in NMe_4NO_3.[11] [e] No complex formation at the experimental conditions. [f] T = 298.2 K, I = 0.10 M in NMe_4NO_3.[37] [g] T = 298.2 K, I = 0.1 M in KCl.[40] [h] T = 298.2 K, I = 0.1 M in NMe_4Cl; the authors report also constants for GaH_2L (log K = 2.43) and GaH_3L (log K = 1.84).[33]

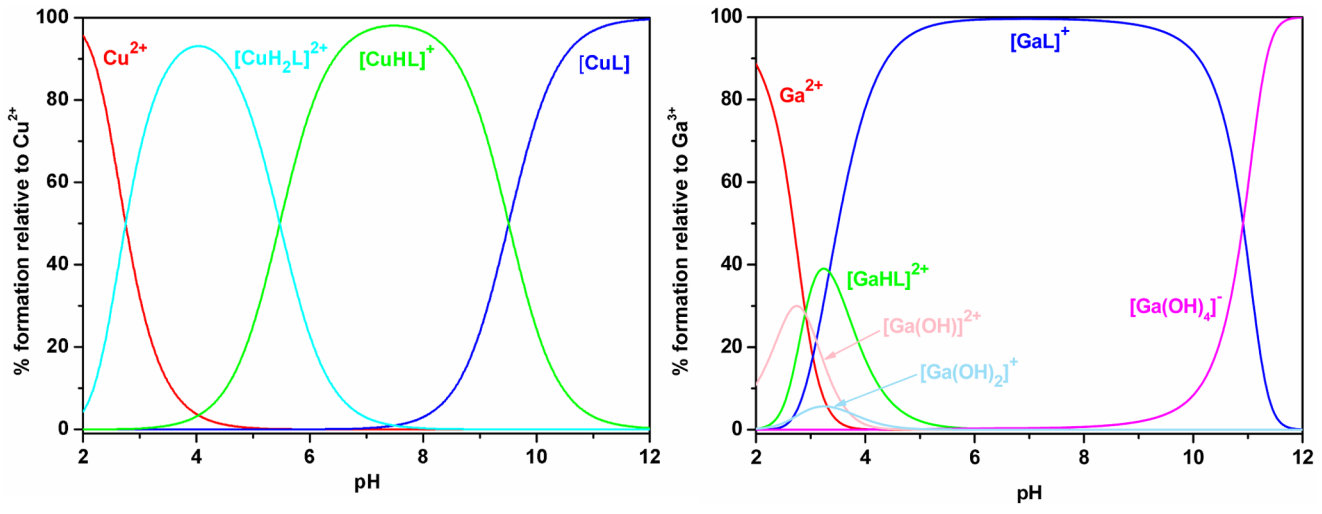

Figure 6. Species distribution diagrams for the complexes of Cu^{2+} and Ga^{3+} with H_2do2ph in aqueous solution at $c_L = c_M = 1.0 \times 10^{-3}$ M.

titrations using long equilibration times. For the complexes of Zn^{2+} and Ca^{2+}, the usual in-cell titrations were used.

The cross-bridged ligand, H_2cb-do2ph, does not form complexes with Ga^{3+} and Ca^{2+} in the mild conditions used. Evidence of the gallium(III) complex formation was only found upon heating; however, some degradation of the complex was also observed along time, as revealed by mass spectrometry. In the case of Cu^{2+}, the slow equilibrium of formation and dissociation of the complex demanded batch titrations at the entire pH region.

The stability constants of the complexes of H_2do2ph and H_2cb-do2ph are high with Cu^{2+} and somewhat less high with

dx.doi.org/10.1021/ic403156h | Inorg. Chem. 2014, 53, 4371−4386

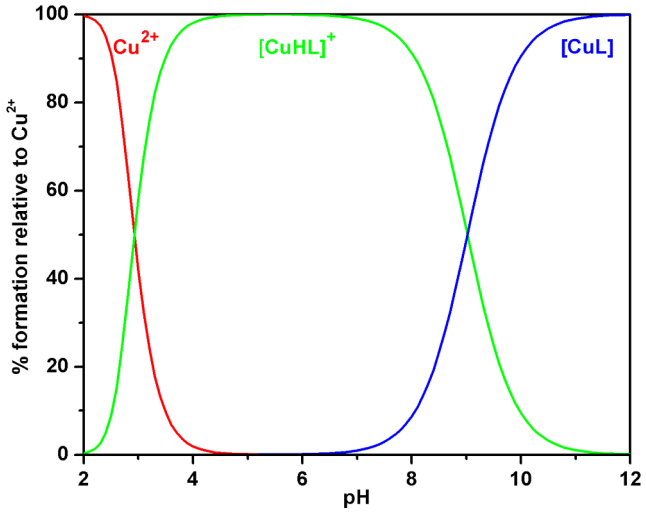

Figure 7. Species distribution diagram for the complexes of Cu^{2+} with H_2cb-do2ph in aqueous solution at $c_L = c_M = 1.0 \times 10^{-3}$ M.

Zn^{2+}, as expected. The most interesting result, however, is the very large stability constant for the complex of H_2do2ph with Ga^{3+} relative to the values of other complexes of the same ligand, and especially when compared to other known ligands such as H_4dota.[33,40] This feature can be explained by the presence of the phenol groups on H_2do2ph, which are known to be particularly suitable for binding hard cations such as Ga^{3+}.[16,41] The high basicity of phenol groups is also responsible for the presence of protonated complex species in solution, and their dominance at neutral or acidic pH, see speciation diagrams in Figures 6 and 7.

However, as is well-known, the comparison of stability constants of metal complexes with ligands of different basicities can be erroneous, and the more correct way consists of comparing them by the conditional constants or the pM = log $[M^{n+}]$ values at a given pH.[42] Consequently, the pM values were determined at physiological pH on the basis of all the constants given in Table 5, and they are collected in Table 6.

Table 6. Calculated pM Values[a] for the Complexes of H_2do2ph, H_2cb-do2ph, and Literature Values of Related Complexes for Comparison

cation	H_2do2ph[b]	H_2cb-do2ph[b]	H_2do2a[c]	H_4dota	do2py[d]	cb-do2py[d]
Cu^{2+}	14.33	13.94	14.91	15.19[e]	17.11	12.63
Zn^{2+}	10.86	8.12	12.01	14.04[e]	14.63	10.70
Ga^{3+}	20.56			17.83;[f] 19.05[g]		

[a]Values calculated at pH = 7.4 for 100% excess of ligand with $[M^{2+}]_{tot} = 1.0 \times 10^{-5}$ M, based on the reported stability constants. [b]This work. [c]From ref 36. [d]From ref 11. [e]From ref 37. [f]From ref 40. [g]From ref 33.

These values highlight the relative strength of the complexes and clearly indicate that the H_2do2ph is a better ligand in comparison to the corresponding cross-bridged one for the complexation of all the studied metal ions, being especially efficient for Ga^{3+} cation. A decrease of stability is expected for complexes of Zn^{2+} relative to those of Cu^{2+} following the trend of Irving–Williams, but the decrease in pM values is more accentuated for the cross-bridged ligand (see the pM values in Table 6).

In conclusion, the $[Ga(do2ph)]^+$ complex presents a surprisingly high pM, to the best of our knowledge the highest one for a complex of a tetraaza macrocyclic derivative, higher than the values reported for the gallium(III) complex of H_4dota.[33,40] However, until now triazamacrocyclic derivatives have been revealed to be the best chelators for the Ga^{3+} ion, especially when three additional arms with oxygen or sulfur donor atoms are appended in order to fulfill the coordinative demand of that metal ion. Indeed, the pGa for the complex of H_3nota is very high (26.41, following Martell et al.,[43] or 23.82, Hermann et al.[44]).

Spectroscopic Characterization of Metal Complexes. The UV–vis spectra of the copper(II) complex of H_2do2ph display a marked pH dependence, see Figure 8. The d–d transition band in the visible region, which is centered at 550 nm at acidic pH, appears at 650 nm at neutral pH and is only slightly intensified at basic pH. At the same time, a shoulder at 395 nm (LMCT band) appears from around neutral pH. On the UV range, the single band at 276 nm at acidic pH gives rise to two separate bands at 234 and 282 nm at neutral pH and then at 238 and 294 nm at basic pH. These results point to the Cu center being bound only by the macrocyclic ring and eventually by a water or solvent molecule at acidic pH, and to the additional coordination of one phenolate group at around neutral pH, suggesting also that the second pendant arm is not bound to the copper center even at basic pH while deprotonating at a value expected for an uncoordinated phenol group.

In contrast with the previous complex, the UV–vis spectra of the copper(II) complex of H_2cb-do2ph display no significant change of λ_{max} of bands in the visible range with the increase of pH (from 5 to 12.2), indicating that at least one phenolate is already coordinated to the metal center at low pH. However, above pH = 9 there is a small increase of absorbance at 410 nm and a small red shift of the band at 605 to 615 nm with a shoulder at 650 nm (the band in the NIR region at 960 nm is maintained along pH change), see Figure 9. In the UV range there are always two bands, one shifting very slightly from 235 to 240 nm and another one shifting from 280 to 293 nm, clearly indicating the deprotonation of the second phenol. These combined features may be the consequence of a slight rearrangement of the ligand around the metal center for the final geometry. This also indicates that the deprotonation of the last phenolate group only occurs at high pH (pK_a = 9.02), suggesting only a weak interaction with the metal center.

The X-band EPR spectra of both complexes exhibit three well-resolved lines of the four expected ones at low field resulting from the interaction of the unpaired electron spin with the copper nucleus, and no superhyperfine splitting due to the coupling with the four nitrogen atoms of the macrocycle was observed. The fourth copper line is partially overlapped by the strong and unresolved band at the high field part of the spectra, see Figure 10. The hyperfine coupling constants (A_i) and g_i values of frozen solutions of the complexes at different pH values, obtained by simulation of the spectra,[45] are listed in Table 7. For all of them the parameters are typical of copper(II) complexes in axially elongated rhombic symmetry and a $d_{x^2-y^2}$ ground state, consistent with elongated rhombic-octahedral, tetragonal, or distorted square-based pyramidal stereochemistries.[46−53] In fact, for all complexes the values for the g_i parameters are $g_z > g_y \approx g_x$ and $g_x \geq 2.04$.

In the complex of H_2do2ph at pH 4 (species $[Cu(H_2do2ph)]^{2+}$), the parameters point to a near axial symmetry, and they are typical of N4O square-pyramidal geometry, following the diagrams of Peisach and Blumberg,[54] as well as the similar values of $[Cu(cyclen)(NO_3)](NO_3)$[55] and of other complexes of cyclen derivatives bearing one pendant arm

dx.doi.org/10.1021/ic403156h | Inorg. Chem. 2014, 53, 4371−4386

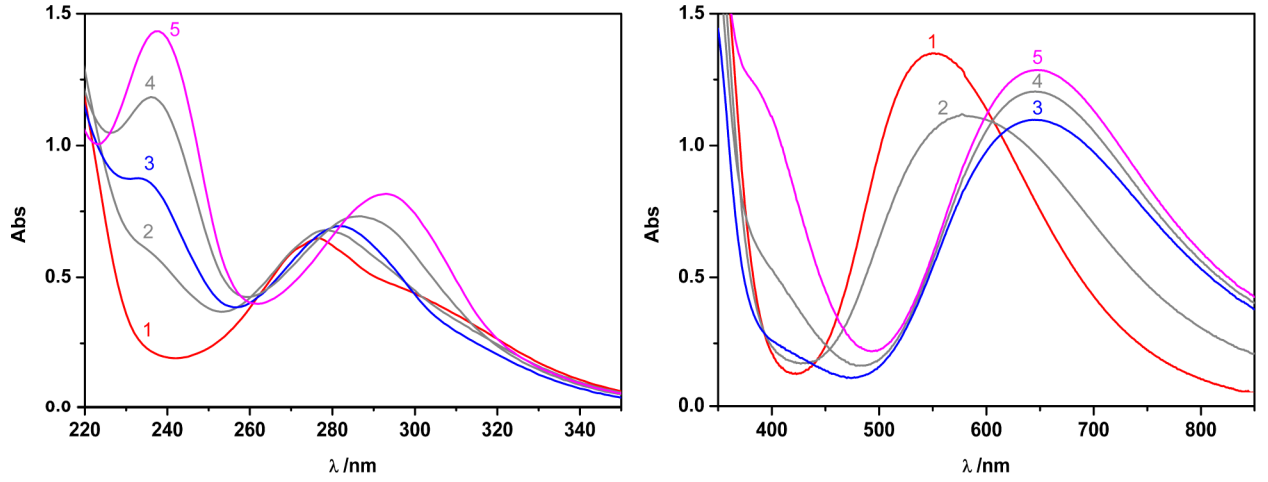

Figure 8. UV and vis spectra of the copper(II) complex of H_2do2ph in aqueous solution at variable pH. (UV: 1−4.1, 2−5.5, 3−7.0, 4−9.5, 5−11.4. Vis: 1−4.0, 2−5.4, 3−7.0, 4−9.2, 5−11.0.)

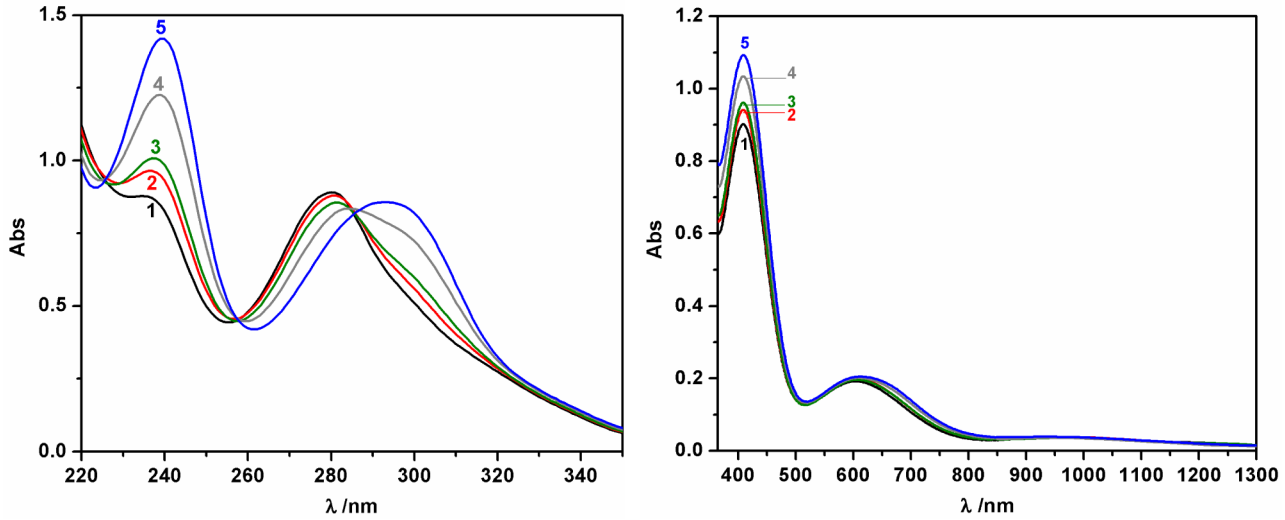

Figure 9. UV and vis−NIR spectra of the copper(II) complex of H_2cb-do2ph in aqueous solution at increasing pH values. (UV: 1−6.2, 2−8.8, 3−9.6, 4−10.0, 5−12.3. vis−NIR: 1−5.0, 2−9.0, 3−9.4, 4−10.3, 5−12.2.)

known as adopting a distorted square pyramidal geometry.[20] Increasing the pH to 7 (species $[Cu(Hdo2ph)]^+$) causes an increase of the g_z and a decrease of the A_z values, which according to the ligand field theory means that the axial ligand field becomes stronger. This fact, together with the simultaneous red-shift of the d−d absorption bands in the electronic spectra, indicates that a coordinated water molecule at the axial position of $[Cu(H_2do2ph)(H_2O)]^{2+}$ ion complex is replaced by the oxygen of a phenolate pendant arm upon deprotonation. Indeed, by potentiometric titration the pK_a value of 5.47 was determined for this deprotonation. This low pK_a value indicates a strong interaction of this phenolate oxygen with the Cu center. Additionally, no significant change of the EPR spectra was observed above pH 7, indicating that the complex preserves the distorted square pyramidal geometry and the same environment. Although from potentiometric and spectrophotometric results it was observed that another phenol group deprotonates at basic pH (pK_a = 9.51), it clearly does not coordinate to the metal center. These structural features of the copper(II) complex of H_2do2ph in aqueous solution are in good agreement with the X-ray diffraction crystal structure determined for the complex $[Cu(Hdo2ph)]ClO_4{\cdot}H_2O$ (see above).

For the copper(II) complex of H_2cb-do2ph, the EPR parameters are identical in the entire pH range studied, indicating that the structure of the complex is very similar at any given pH. The potentiometric studies revealed that the complex is formed at low pH and only a deprotonation of one phenolate was observed at high pH (pK_a = 9.02, see Table 5), indicating that one of the phenol groups deprotonates at low pH and is strongly bound to the metal center. In a comparison of the EPR parameters of this complex with those of $[Cu(Hdo2ph)]^+$ or [Cu(do2ph)], an increase of the g_z and a decrease of the A_z values are observed, indicating a stronger axial ligand field or/and a weaker equatorial ligand field. These features suggest a distorted tetragonal geometry with a water molecule completing the hexacoordination at low pH, which is replaced by the second phenolate group weakly bound at pH > 9 (pK_a = 9.02, which is lower than the corresponding pK_a = 10.34 of the free ligand, suggesting a weak interaction). In spite of our efforts, it was unfortunately not possible to obtain crystals of this complex with appropriate quality for X-ray determination. However, the structure of the complex with the related ligand H_2cb-do2nph $[Cu(cb\text{-}do2nph)]$[20] exhibited a distorted axial elongated octahedral geometry with a N3O equatorial plane and NO axial

dx.doi.org/10.1021/ic403156h | Inorg. Chem. 2014, 53, 4371−4386

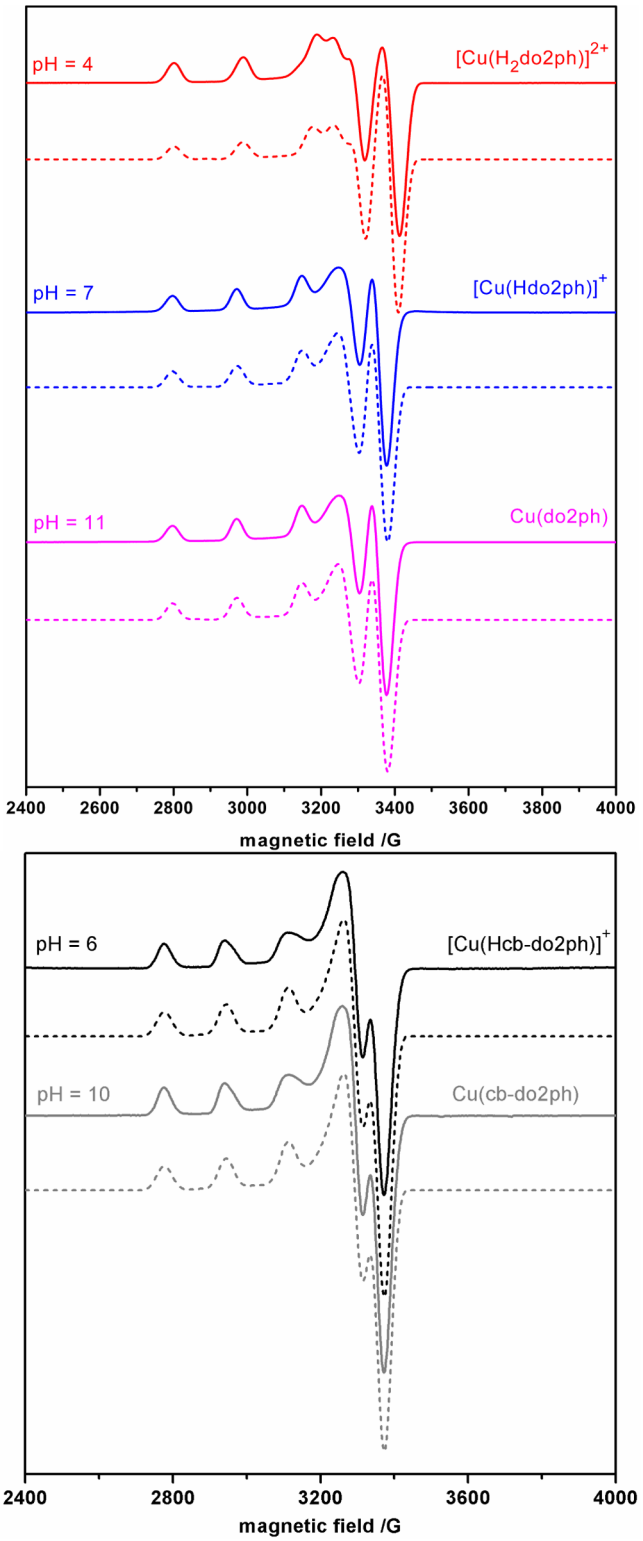

Figure 10. X-band EPR spectra of the copper(II) complexes of H_2do2ph (top) and H_2cb-do2ph (bottom) in frozen water/ethylene glycol (1:1 v/v) solutions of variable pH recorded at 90 K, and the corresponding simulated spectra in dashed lines. Microwave power of 2.0 mW, modulation amplitude of 1.0 mT, and frequency (υ) of 9.5 GHz.

bonds, with the axial O-phenolate being at a distance of 2.343 Å. The EPR parameters of [Cu(do2ph)] being intermediate between those of [Cu(cb-do2nph)][20] and [Cu(do2ph)] point to a structure similar to that of [Cu(cb-do2nph)] with a longer distance to the axial phenolate.

To get an insight into the structures of zinc(II) and gallium(III) complexes of H_2do2ph, NMR spectra of deuterated water solutions were recorded at relevant pH values. The ^{1}H spectra of the zinc(II) complex are quite simple and similar at pH 7 and 11, which is indicative of a single and very symmetric species in solution, see Figure S8 of Supporting Information. They display only three resonances for the macrocyclic ring and another five for the two pendant arms, indicating that the arms are magnetically equivalent. The sharp singlet at 3.83 ppm assigned to the methylene (N−CH_2−Ar) protons of the pendant arms means that they are in fast exchange on the NMR time scale and thus suggests that there probably only exists a weak binding of the phenolate groups to the cation. For the gallium(III) complex, the ^{1}H spectra are much more complicated, as there are many multiplets for the macrocyclic ring and the pendant arms both at pH 4 and 9, see Figure S9 of Supporting Information. The most distinctive features of the spectra are three different multiplets in the range 3.9−5.0 ppm that are assigned to the methylene protons of the pendants (three pairs of doublets from the AB spin systems formed by inequivalent geminal protons), which means that all the phenolate groups bind strongly to the cation. The ^{13}C spectrum of the complex is also complicated, displaying two sets of resonances apparently corresponding to one major (*M*) and one minor (*m*) isomers (Figure S10 of Supporting Information), which could be identified with the help of standard 2D COSY and HMQC experiments (Figures S11 and S12 of Supporting Information). The *M* isomer has 7 different carbon atoms assigned to the macrocyclic ring (41−59 ppm range) and 2 assigned to the methylene carbon atoms of the pendant arms (∼61 ppm) while the *m* isomer has only 4 macrocyclic carbon atoms and one for the pendants, which points to an effective C_1 symmetry for the former isomer and a C_2 symmetry for the latter one. The combined NMR data for the gallium(III) complex point to two isomers coexisting in solution such that one of them has magnetically inequivalent pendant arms yielding two of the methylene multiplets, and the other one has equivalent pendants yielding a single multiplet. ^{1}H spectra were also performed at variable temperatures up to 90 °C in D_2O and 110 °C in DMSO-d_6 (Figures S13 and S14 of Supporting Information), but although an increase of the linewidths of the multiplets of the pendants multiplets was visible, that reflects conformational exchange processes taking place, and no final interconversion between the two isomers was observed. This indicates a dynamic process with high activation barrier.

Unfortunately, it was not possible to perform NMR measurements of the diamagnetic Zn^{2+} complexes of H_2cb-do2ph due to its slow formation. However, it is interesting to note that the complex of this ligand with Zn^{2+} has a deprotonation at lower pH than the one of the copper(II) complex (pK_a = 6.69), suggesting the coordination of both phenolate groups to the Zn center to form a 6-coordinate complex which is completely formed around pH 8, see Supporting Information Figure S7.

Kinetic linertness of Copper(II) and Gallium(III) Complexes of H_2do2ph and H_2cb-do2ph. The kinetic inertness of metal complexes is one of the most important properties to consider for the possible application in nuclear medicine, since it is crucial that complexes do not dissociate during their residence time in the patient body. Determination of the half-life times for complexes in acidic or basic media is a commonly accepted method to ascertain their inertness in comparison with other known complexes.

dx.doi.org/10.1021/ic403156h | Inorg. Chem. 2014, 53, 4371−4386

Table 7. Visible and X-Band EPR Spectroscopic Data of the Copper(II) Complexes of H_2do2ph and H_2cb-do2ph

complex	pH	UV−vis−NIR[a] λ_{max} /nm (ε/M^{-1} cm^{-1})	X-band EPR[b] g_z	g_y	g_x	A_z[c]	A_y[c]	A_x[c]
$[Cu(H_2do2ph)(H_2O)]^{2+}$	4	276 (6.6×10^3); 550 (312)	2.191	2.053	2.040	191	25	22
$[Cu(Hdo2ph)]^{+}$	7	234 (9.0×10^3); 282 (7.2×10^3); 650 (254)	2.207	2.071	2.042	180	13	<10
[Cu(do2ph)]	11	238 (1.5×10^4); 294 (8.4×10^3); 395 (266); 650 (298)	2.207	2.071	2.042	180	13	<10
$[Cu(Hcb-do2ph)]^{+}$	6	235 (8.8×10^3); 280 (8.9×10^3); 410 (546); 605 (134); 960 (39)	2.233	2.061	2.037	173	16	<10
[Cu(cb-do2ph)]	10	239 (12.3×10^3); 285 (8.3×10^3); 410 (610); 615 (141); 650 (sh); 960 (39)	2.233	2.061	2.037	173	16	<10
$[Cu(cyclen)(NO_3)]NO_3$[d]		500 (250)	2.198	2.057		184	24	

[a]In aqueous solution, recorded at 298 K. [b]In H_2O/ethylene glycol (1:1 v/v) solution, recorded at 90 K at microwave power 2.0 mW and frequency (ν) 9.5 GHz; parameters obtained by spectral simulation. [c]Values of $A \times 10^4$ in cm^{-1}. [d]From ref 55.

The acid-assisted dissociation of the copper(II) complexes of H_2do2ph and H_2cb-do2ph was studied by vis spectrophotometry under pseudo-first-order conditions in 1 M HCl solutions at different temperatures. The calculated half-life times ($t_{1/2}$) are presented in Table 8 together with literature values for related complexes. The first striking observation from the results obtained is that the complex of the cross-bridged H_2cb-do2ph derivative is surprisingly much less inert than that of H_2do2ph. That is even more significant taking into account that the inertness of the complex of H_2cb-do2ph is reasonably high when compared to other complexes of cross-bridged cyclen derivatives, thus indicating that it is actually the complex of H_2do2ph that is more inert than expected. The temperature dependences of the rate constants (k_{obs}) determined for both complexes are shown in the Arrhenius plots obtained for each dissociation reaction (Figure S15 of Supporting Information).

Table 8. Half-Life Times ($t_{1/2}$) for the Acid-Assisted Dissociation of the Copper(II) Complexes of H_2do2ph and H_2cb-do2ph and Literature Values for Complexes of Related Ligands

copper(II) complex of L	conditions [HCl]/M (T/K)	$t_{1/2}$/min	ref
H_2do2ph	1 (298.2)	1296	this work
	1 (310.2)	358	this work
	1 (333.2)	28.5	this work
	1 (363.2)	2.3	this work
H_2cb-do2ph	1 (298.2)	393	this work
	1 (303.2)	214	this work
	1 (310.2)	86.1	this work
	1 (333.2)	6.6	this work
	1 (363.2)	0.5	this work
H_2do2nph	1 (298.2)[a]	10.9	20
H_2cb-do2nph	1 (298.2)[a]	46.1	20
H_2cb-do2a	1 (303.2)	240	9
cb-do2py	1 (303.2)	52	11
cyclen	5 (303.2)	<3	3
H_4dota	5 (303.2)	<3	3

[a]Determined in DMSO−H_2O (9:1 v/v) solutions due to poor solubility of the complexes in water.

The base-assisted dissociation of the gallium(III) complex of H_2do2ph was also studied by ^{71}Ga NMR spectroscopy in buffered aqueous solutions at pH = 11. The dissociation was followed by integration of the increasing resonance of the $[Ga(OH)_4]^-$ species that is formed at basic pH by the metal released from the complex. The half-life of 54 min found for the complex is much lower than the best known gallium(III) complex, but still moderately high when compared to those of other cyclen derivatives (Table 9).[33,56] Nonetheless, it is of a magnitude similar to the half-life of the ^{68}Ga isotope (67.7 min) that is useful for applications in PET imaging.

Table 9. Half-Life Times for the Base-Assisted Dissociation of the Gallium(III) Complex of H_2do2ph and Literature Values for Related Complexes

ligand	pH (T/K)	$t_{1/2}$/min	ref
H_2do2ph	11 (298.2)	54	this work
H_4dota	10 (298.2)	372	33
H_3do3a1am[a]	10 (298.2)	43	33
H_6trap-Pr[b]	11 (298.2)	3600	56

[a]1,4,7,10-Tetraazacyclododecane-1,4,7-tris-acetic acid-10-acetamide. [b]1,4,7-Triazacyclononane-1,4,7-tris[methyl(2-carboxyethyl)phosphinic acid].

Electrochemical Behavior of the Copper(II) Complexes of of H_2do2ph and H_2cb-do2ph. The efficiency of copper complexes for radiopharmaceutical applications can also be limited by bioreduction to copper(I) complex followed by demetalation in case the ligand is not able to stabilize the reduced copper species. However, most copper(II) complexes of polyazamacrocyclic derivatives have reduction potentials that are well below the estimated −0.40 V (NHE) threshold for typical bioreductants.[3] Therefore, the copper(II) complexes of H_2do2ph and H_2cb-do2ph were investigated by cyclic voltammetry (CV) in 0.10 M aqueous NaOAc at pH 10.0 and 9.4, respectively, see Figure S16 of Supporting Information. The reduction of both complexes is irreversible with the cathodic waves at −912 and −941 mV (Ag/AgCl, scan rate 100 mV/s) for [Cu(do2ph)] and [Cu(cb-do2ph)], respectively. However, for [Cu(do2ph)] one anodic peak at −568 mV (Ag/AgCl, scan rate 100 mV/s) on the reverse sweep was observed. It seems that the reduced complex may exist as a mixture of at least two species in fast equilibrium. These species may consist of four- and five-coordinate Cu(I) complexes, as also observed for other macrobicyclic complexes.[57,58] Such irreversibility is generally attributed to the lack of ability of cyclen derivatives to accommodate and stabilize the Cu^+ ion in its cavity, in contrast with their cyclam counterparts.[9] Consequently, upon reduction of the Cu^{2+} center to Cu^+ in the studied complexes, a topological reorganization, demetalation, and/or disproportionation may occur, indicating that their rigid backbones and small cavities do not appear to be able to adapt well to the coordination requirements of Cu^+ in order to stabilize it.

CONCLUSIONS

In this work two novel cyclen-based metal chelators are reported containing two *trans*-methyl phenol pendant arms,

dx.doi.org/10.1021/ic403156h | Inorg. Chem. 2014, 53, 4371−4386

H_2do2ph and H_2cb-do2ph, where the latter one contains also an ethylene cross-bridge, aiming for possible use of their metal complexes in nuclear medicine. Studies of the acid−base properties of both compounds showed that H_2do2ph displays unusual dissimilar basicity of the phenolic pendant arms, while the cross-bridged H_2cb-do2ph derivative has a marked "proton sponge" behavior that is common in small polyamine cages. These basicity features were found to play a crucial role in the metal binding properties of the compounds.

The copper(II) complexes of H_2do2ph and H_2cb-do2ph have similarly high thermodynamic stability, which in the case of H_2do2ph is somewhat lower than for other cyclen derivatives such as H_4dota. This may be assigned to the coordination role of the phenol pendants in the structure of both complexes, as the spectroscopic studies and the X-ray structure of the complex of H_2do2ph showed that one phenolate arm is not coordinated to the copper center while for the H_2cb-do2ph the spectroscopic data suggest a hexacoordinated complex in which one of the phenolate groups is only weakly bound to the metal center. More important and rather surprising is the fact that the copper complex of H_2do2ph is approximately 4 times more inert that that of H_2cb-do2ph, being more inert than the complexes of most other cyclen derivatives. All of the above features indicate that H_2do2ph may be an interesting ligand for the complexation of copper(II) radioisotopes in medicinal applications.

The gallium(III) complex of H_2do2ph has a very high thermodynamic stability, which translates to a pM value (20.79) that is better than for H_4dota. This means that H_2do2ph is the best known tetraaza macrocyclic derivative for complexation of Ga^{3+} cation. The octahedral complex $[Ga(do2ph)]^+$ has additionally shown an appropriate inertness toward base-assisted dissociation, making it a promising candidate for applications with gallium(III) radioisotopes in medicine if the problem of a rather slow complexation rate can be overcome.

In contrast with the behavior of all reported cross-bridged compounds, our studies revealed that the *trans*-bismethylphenol cyclen derivative H_2do2ph is the best ligand for the coordination of both Cu^{2+} and Ga^{3+} cations in aqueous solution, not only from the larger pM values but also from the kinetic inertness of its complexes when compared with its corresponding cross-bridged one. In fact, to the best of our knowledge this is the first case where the copper(II) complex of the cross-bridged derivative (H_2cb-do2ph) is much less inert than that of its non-cross-bridged counterpart.

EXPERIMENTAL SECTION

Materials and Methods. Cyclen (1,4,7,10-tetraazacyclododecane) was obtained from CheMatech. All solvents and chemicals were obtained from commercial sources as reagent grade quality and used as received. 1,7-Bis(benzyloxycarbonyl)-tetraazacyclododecane (**2**), cyclen-glyoxal (**1**), and (bromomethy1) phenyl acetate were prepared by literature procedures.[26,59,60] The ^{1}H and ^{13}C{^{1}H} NMR spectra were recorded on a Bruker Avance II+ 400 (^{1}H at 400.13 MHz and ^{13}C at 100.61 MHz) or a Bruker Avance DRX 300 (^{1}H at 300.13 MHz) spectrometer at probe temperature of 298.2 K. Chemical shifts (δ) are given in ppm and coupling constants (J) in Hz. 3-(Trimethylsilyl) propionic acid sodium salt was used as internal references for ^{1}H NMR spectra in D_2O. Assignments are based on peak integration and multiplicity and on 2D HMQC experiments (see Supporting Information). Microanalyses were carried out by the ITQB Analytical Services Unit. The electronic absorption spectra were recorded on a UNICAM UV−vis spectrophotometer model UV-4. EPR spectra were recorded on a Bruker EMX 300 spectrometer equipped with continuous-flow cryostat for liquid nitrogen, operating at the X-band.

Caution! *Although no problems were encountered during this work with the perchlorate salts, these compounds should be considered potentially explosive.*

*Cyclen-glyoxal trans-Bis(2-methylphenyl acetate) Diammonium Bromide, **2**.* A solution of 2-(bromomethy1)phenyl acetate (2.133 g, 9.3 mmol) in MeCN (15 mL) was added dropwise over 30 min to a magnetically stirred solution of cyclen glyoxal **1** (0.611 g, 3.1 mmol) in MeCN (15 mL). The mixture was left under stirring at room temperature (rt) for 7 days. A precipitate formed which was filtered and washed with MeCN, followed by diethyl ether. The compound was dried in an oven at 55 °C and used without purification in the next step (1.950 g, 95%). ^{1}H NMR (400 MHz, D_2O): δ 7.75 (2 H, d, J = 8.0 Hz, 3-H, Ar), 7.71 (2 H, t, J = 8.0 Hz, 5-H, Ar), 7.51 (2 H, t, J = 8.0 Hz, 2-H, Ar), 7.42 (2 H, d, J = 8.0 Hz, 4-H, Ar), 5.03, 4.73 (4 H, ABq, J_{AB} = 13 Hz, CH_2ph) 4.90 (2 H, s, C*H*-bisaminal), 4.35−3.10 (16 H, m, CH_2−ring), 2.48 (6 H, s, CH_3) ppm. ^{13}C NMR (100 MHz, D_2O): δ 172.1 (C═O), 150.2, 134.5, 133.2, 127.4, 124.0, 118.7 (Ar), 78.3 (CH-bisaminal), 61.0 (CH_2ph), 55.7, 55.1, 45.9, 43.1 (C-ring), 21.0 (CH_3) ppm.

H_2cb-do2ph. The diammonium bromide salt **2** (1.950 g, 2.83 mmol) was suspended in EtOH/H_2O 90:10 (50 mL), and solid $NaBH_4$ (1.071 g, 28.3 mmol) was added in small portions. After the addition was completed, the mixture was left under stirring at rt for 1 day. The suspended solid was filtered and discarded. The mother liquor was evaporated to dryness, and the residue was redissolved in 1 M KOH (40 mL) and left stirring overnight at 70 °C. The solution was transferred to a separating funnel and the pH adjusted to 9−10 with diluted $HClO_4$. The white precipitate formed was extracted with $CHCl_3$ (4 × 50 mL), and the organic phases were dried with anhydrous Na_2SO_4, filtered, and evaporated to dryness. The solid was suspended in water acidified to pH 3−4 with diluted $HClO_4$ after which the mixture was heated to 65 °C and left stirring for 3 days (at this temperature the solid is completely dissolved). The solution was allowed to reach rt, and the white precipitate formed was filtered and dried under vacuum (0.639 g, 37%). Mp 170 °C (decomp). ^{1}H NMR (400 MHz, D_2O): δ 7.43−6.95 (8 H, m, Ar), 4.47 (4 H, s, CH_2ph), 3.80−2.74 (16 H, NCH_2CH_2N-ring), 2.86 (4 H, s, NCH_2CH_2N-bridge) ppm. ^{13}C NMR (100 MHz, D_2O): δ 155.3 (C1), 132.8 (C4, C5), 132.2 (C6), 121.1, 116.7 (C2, C3), 56.4, 53.2 (CH_2-ring), 55.6 (CH_2ph), 46.8 (CH_2-bridge) ppm. Anal. Calcd for $C_{24}H_{36}N_4O_2{\cdot}2ClO_4$: C, 47.1; H, 5.9; N, 9.2%. Found: C, 47.1; H, 6.2; N, 9.0%. ESI-MS (H_2O/MeOH, 1:1) m/z: 411.1 (100) $[M + H]^+$, 305.1 (4) $[M - C_7H_7O^+ + 2H]^+$

*1,7-Bis(benzyloxycarbonyl)-4,10-bis(2-methylphenyl acetate)-tetraazacyclododecane, **4**.* A solution of 2-(bromomethy1)phenyl acetate (2.5 g, 10.9 mmol) in MeCN (5 mL) was added dropwise to a magnetically stirred mixture of 1,7-bis(benzyloxycarbonyl)-tetraazacyclododecane **3** (1.922 g, 4.4 mmol) and K_2CO_3 (1.33 g, 9.6 mmol) in MeCN (15 mL). The mixture was left under stirring at 40 °C for 3 days and at 60 °C for 4 days. The precipitate formed upon cooling to rt was filtered, dissolved in $CHCl_3$, and washed with H_2O. The organic phase was dried with anhydrous Na_2SO_4, filtered, and evaporated to dryness. The pure compound was obtained after flash column chromatography on silica gel using $CHCl_3$/ethyl acetate (8:2) as eluent (1.750 g, 55%). ^{1}H NMR (400 MHz; $CDCl_3$): δ 7.40−6.95 (16 H, m, Ar), 4.90 (4 H, s, CH_2bz), 3.51 (4 H, s, CH_2phac), 3.38 (8 H, m, NCH_2CH_2N), 2.65 (8 H, m, NCH_2CH_2N), 2.28 (6 H, s, CH_3) ppm. ^{13}C NMR (100 MHz, $CDCl_3$): δ 169.3 (C═O), 156.5, 149.6, 136.8, 128.5, 128.2, 128.0, 126.1, 122.4 (Ar), 67.1 (CH_2bz), 60.5 (CH_2phac), 54.7, 46.9 (C-ring), 21.1 (CH_3) ppm.

H_2do2ph. 1,7-Bis(benzyloxycarbonyl)-4,10-bis(2-methylphenyl acetate)-tetraazacyclododecane **4** (1.750 g, 2.4 mmol) was suspended in 33% HBr (10 mL) and left stirring for 1 h at rt. Diethyl ether was added (50 mL), and the precipitate formed was filtered. The solid was dissolved in NaOH 0.1 M (170 mL) and left stirring at rt overnight. The solution was transferred to a separating funnel and extracted with $CHCl_3$ (5 × 60 mL). The aqueous phase was concentrated to about 40 mL, the pH was adjusted to ∼9 with diluted $HClO_4$, and a second extraction was carried out with $CHCl_3$ (4 × 20 mL). The combined

dx.doi.org/10.1021/ic403156h | *Inorg. Chem.* 2014, 53, 4371−4386

organic phases were dried with anhydrous Na_2SO_4, filtered, and evaporated to dryness. The product was recrystallized from boiling MeCN. The desired compound was obtained as a crystalline solid (0.940 g, 56%). Mp 169 °C (decomp). ^{1}H NMR (400 MHz, $CDCl_3$): δ 7.10 (2 H, td, J = 8.0 Hz, 1.7 Hz, 3-H, Ar), 6.91 (2 H, dd, J = 7.4 Hz, 1.3 Hz, 5-H, Ar), 6.86 (2 H, dd, J = 8.1 Hz, 1.0 Hz, 2-H, Ar), 6.70 (2 H, td, J = 7.4 Hz, 1.0 Hz, 4-H, Ar), 4.94 (bs, OH), 3.71 (s, 4 H, CH_2ph), 2.70−2.60 (16 H, $NHCH_2CH_2N$) ppm. ^{13}C NMR (100 MHz, $CDCl_3$): δ 157.8 (C1), 129.0 (C3, C5), 122.9 (C6), 119.2 (C4), 116.9 (C2), 60.4 (CH_2ph), 53.6 ($NHCH_2$), 47.6 (CH_2N) ppm. Anal. Calcd for $C_{22}H_{32}N_4O_2$: C, 68.7; H, 8.4; N, 14.6%. Found: C, 68.7; H, 8.5; N, 14.2%. ESI-MS (H_2O/MeOH, 1:1) m/z: 107.0 (5) $[C_7H_7O]^+$, 279.1 (25) $[M - C_7H_7O^+ + 2H]^+$, 385.1 (100) $[M + H]^+$.

[Cu(do2ph)]. An aqueous 0.1 M solution of $Cu(ClO_4)_2$ (0.52 mL, 0.052 mmol) was added to a solution of H_2do2ph (20 mg, 0.052 mmol) in water (15 mL), the pH was neutralized with diluted aqueous KOH, and the blue solution was stirred overnight at rt. The solution was evaporated to dryness, the complex was dissolved in absolute ethanol, and the insoluble matter was filtered off. The previous step was repeated until no more insoluble matter was observed. The resulting solution was evaporated, and the solid obtained was dried under vacuum to yield the complex in the monoprotonated form (21 mg, 71%). Anal. Calcd for $CuC_{22}H_{31}N_4O_2{\cdot}ClO_4{\cdot}3H_2O$: C, 44.0; H, 6.2; N, 9.3%. Found: C, 44.0; H, 5.8; N, 9.2%. ESI-MS (H_2O/MeOH, 1:1) m/z: 446.1 (100) $[Cu(Hdo2ph)]^+$, 223.4 (10) $[Cu(H_2do2ph)]^{2+}$, 554.9 (10) $([Cu(H_2do2ph)]ClO_4)^+$.

[Cu(cb-do2ph)]. An aqueous 0.1 M solution of $Cu(ClO_4)_2$ (1.68 mL, 0.168 mmol) was added to a solution of H_4cb-do2ph$(ClO_4)_2$ (103 mg, 0.168 mmol) in water (50 mL), the pH was neutralized with diluted aqueous KOH, and the dark green solution was stirred at 50 °C for 2 h. The solution was evaporated to dryness, the complex was dissolved in methanol, and the insoluble matter was filtered off. This procedure was repeated until no more precipitation was observed. The dark green solid obtained was dried in vacuum until constant mass (71 mg, 74%). Anal. Calcd for $CuC_{24}H_{33}N_4O_2{\cdot}ClO_4$: C, 50.3; H, 5.8; N, 9.8%. Found: C, 50.0; H, 5.9; N, 10.1%. ESI-MS (H_2O/MeOH, 1:1) m/z: 472.1 $[CuH(cb\text{-}do2ph)]^+$.

[Ga(do2ph)]NO$_3$. An aqueous 0.022 M $Ga(NO_3)_3$ (4.6 mL) solution was added to H_2do2ph (38.4 mg, 0.1 mmol) dissolved in water (30 mL), the pH was slowly raised to 9.0 by addition of 0.1 M KOH, and the solution was left stirring at 60 °C overnight. The pH was readjusted to 9.0, the solution was concentrated in the evaporator and was left cooling overnight. The precipitate obtained was filtered and dried in vacuum until constant mass (27 mg, 53%). Anal. Calcd for $GaC_{22}H_{30}N_4O_2{\cdot}NO_3$: C, 51.4; H, 5.9; N, 13.6%. Found: C, 51.3; H, 6.2; N, 13.5%. ESI-MS (H_2O) m/z: 451.1 $[Ga(do2ph)]^+$.

X-ray Crystallography. Crystals of H_2do2ph were prepared by slow overnight crystallization of a concentrated solution of the compound prepared in hot MeCN. Crystals of $[Cu(Hdo2ph)]ClO_4{\cdot}H_2O$ were obtained by addition of 5 M $NaClO_4$ to an aqueous solution of the complex, after 2 days of slow evaporation at rt. Crystals of $[Ga(do2ph)]NO_3{\cdot}2H_2O$ were prepared by slow evaporation at rt over 2 days of a concentrated solution of the complex. Single crystal X-ray data of H_2do2ph was collected on an in-house Bruker AXS Microstar imaging plate detector (X8 PROTEUM diffractometer), with graphite monochromated Cu-Kα radiation (λ = 1.54 Å). The selected crystal was positioned at 50 mm from the CCD and exposed for 20s per frame. Data reduction of the data set was carried out using the SAINT-NT from Bruker AXS, with a multiscan absorption correction (SADABS). The crystal only diffracted up to 1.25 Å resolution, with a reflection to parameters ratio of 4.8, which resulted in a low bond precision for C−C. Attempts were made to collect higher resolution data, either by improving crystal quality and/or by collecting data on a Bruker AXS-KAPPA APEX II diffractometer with graphite monochromated Mo-Kα radiation, but were unsuccessful. Nevertheless, it was possible to solve and determine the structure of the compound. The structure was solved with SHELXS[61] by direct methods and refined on F^2 using full-matrix least-squares with SHELXL,[61] included in the WINGX-Version 1.70.01[62] package of programs. All non-hydrogen atoms were refined with anisotropic thermal parameters. The majority of the hydrogen atoms were introduced at calculated positions and refined using the riding model, except for the hydrogen atoms bound to the macrocycle nitrogens and to oxygen atoms that were positioned according to electron density peaks identified in the difference Fourier maps and refined with individual isotropic temperature parameters. Single crystal X-ray data of $[Cu(Hdo2ph)]ClO_4{\cdot}H_2O$ and of $[Ga(do2ph)]NO_3{\cdot}2H_2O$ were collected on a Bruker AXS-KAPPA APEX II diffractometer, with graphite monochromated Mo-Kα radiation (λ = 0.710 69 Å). The selected crystals of each compound,were positioned at 40 mm from the CCD and exposed for 10 s per frame. Data reduction of each data set was carried out using the SAINT-NT from Bruker AXS, with a multiscan absorption correction (SADABS). The structures were solved with SHELXS[61] by direct methods and refined on F^2 using full-matrix least-squares with SHELXL,[61] included in the WINGX-Version 1.70.01[62] package of programs. All non-hydrogen atoms were refined with anisotropic thermal parameters. The majority of the hydrogen atoms were introduced at calculated positions and refined using the riding model, except for the hydrogen atoms bound to the macrocycle nitrogens and to oxygen atoms that were positioned according to electron density peaks identified in the difference Fourier maps and refined with individual isotropic temperature parameters. The analysis of the difference Fourier maps has also allowed the identification of solvent and counterion molecules in both complexes, although in the case of $[Cu(Hdo2ph)]{\cdot}ClO_4{\cdot}H_2O$ the hydrogen atoms from the water molecule could not be identified in the difference Fourier maps. Data and refinement statistics for both complexes are listed in Table 10.

Spectroscopic Studies. UV−vis−NIR spectra of the copper(II) complexes of H_2do2ph and H_2cb-do2ph and UV spectra of the ligands alone were recorded at 298.2 K in aqueous solutions of variable pH. Samples were prepared at 7.5×10^{-5} M for H_2do2ph, and at 9.2×10^{-5} M for H_2cb-do2ph; at 4.3×10^{-3} M (vis) or 9.7×10^{-5} M (UV) for the complex of H_2do2ph, and at 1.1×10^{-3} M (vis) or at 9.3×10^{-5} M (UV) for that of H_2cb-do2ph. The pH of the solutions was adjusted with diluted aqueous KOH or HNO_3. Samples for EPR spectroscopy were prepared from the previous solutions, by addition of ethylene glycol/water to a 1:1 (v/v) final mixture. These samples were frozen, and X-band EPR spectra were acquired at 90 K, recorded at a microwave power of 2.0 mW and a frequency (ν) of 9.5 GHz. The EPR spectra were simulated with the SpinCount software,[45] in order to obtain the relevant parameters. NMR samples of the zinc(II) and gallium(III) complexes of H_2do2ph were prepared in D_2O and DMSO-d_6 at ca. 2×10^{-3} M by mixing equimolar amounts of H_2do2ph and the relevant metal nitrate in aqueous solutions, followed by adjustment of pH, evaporation to dryness, and redissolution in the deuterated solvent. ^{1}H, ^{13}C, and 2D homo- and heteronuclear NMR spectra were run at 298 K with the chemical shifts referenced to the solvent residual peak. ^{1}H NMR spectra were also run at variable temperature in both D_2O and DMSO-d_6.

Potentiometric Measurements. *Equipment and Work Conditions.* The potentiometric setup for conventional titrations consisted of a 50 mL glass-jacketed titration cell sealed from the atmosphere, connected to a separate glass-jacketed reference electrode cell by a Wilhelm type salt bridge containing 0.10 M KNO_3 solution. An Orion 720A measuring instruments fitted with a Metrohm 6.0123.100 glass electrode and a Metrohm 6.0733.100 Ag/AgCl reference electrode was used for the measurements. The ionic strength of the experimental solutions was kept at 0.10 ± 0.01 M with KNO_3, and temperature was maintained at 298.2 ± 0.1 K using a PolyScience 910 thermostat. Atmospheric CO_2 was excluded from the titration cell during experiments by slightly bubbling purified nitrogen on the experimental solution. Titrant solutions were added through capillary tips at the surface of the experimental solution by a Metrohm Dosimat 665 automatic buret. Titration procedure is automatically controlled by software, allowing for long unattended experimental runs. In cases where automatic titrations could not be performed, out-of-cell titrations were carried out instead and the electromotive force was measured with a Metrohm 6.0234.100 combined pH electrode previously calibrated by titration.

Measurements. Purified water was obtained from a Millipore Milli-Q demineralization system. Stock solutions of H_2do2ph and

dx.doi.org/10.1021/ic403156h | Inorg. Chem. 2014, 53, 4371−4386

Table 10. Crystal Data and Selected Refinement Details for H_2do2ph and Respective Copper(II) and Gallium(III) Complexes

	H_2do2ph	[Cu(Hdo2ph)]ClO_4·H_2O	[Ga(do2ph)]NO_3·2H_2O
empirical formula	$C_{22}H_{32}N_4O_2$	$C_{22}H_{33}ClCuN_4O_7$	$C_{22}H_{34}GaN_5O_7$
fw	384.51	564.52	550.26
T (K)	150	150	150
cryst syst	monoclinic	monoclinic	monoclinic
space group	$P2_1/n$	$P2_1/n$	$P2_1/c$
cell dimensions (Å, deg)	a = 10.5471(13)	a = 16.5986(6)	a = 10.0897(3)
	b = 14.1489(18)	b = 8.9107(3)	b = 13.0832(4)
	c = 14.4577(19)	c = 16.7580(6)	c = 17.9815(7)
	β = 102.244(4)	β = 103.202(2)	β = 92.5540(10)
V (Å^3)	2108.4(5)	2413.09(15)	2371.30(14)
Z	4	4	4
ρ_{calc} (g cm^{-3})	1.211	1.548	1.541
μ (mm^{-1})	0.079	1.067	1.214
F(000)	832	1172	1152
reflns collected	8291	26 001	23 653
indep	1232	7353	7241
reflns [$I > 2\sigma(I)$]	1195	5756	5616
no. variables	258	328	340
R_{int}	0.0392	0.0522	0.0465
final R indices [$F^2 > 2\sigma(F^2)$][a]	R_1 = 0.0589	R_1 = 0.0725	R_1 = 0.0418
	wR_2 = 0.1503	wR_2 = 0.1951	wR_2 = 0.1053
R indices (all data)[a]	R_1 = 0.0600	R_1 = 0.0916	R_1 = 0.0600
	wR_2 = 0.1512	wR_2 = 0.2044	wR_2 = 0.1153

[a] $R_1 = \Sigma||F_o| - |F_c||/\Sigma|F_o|$; $wR_2 = \{\Sigma[w(F_{o0}^2 - F_c^2)^2]/\Sigma[w(F_o^2)^2]\}^{1/2}$.

H_2cb-do2ph were prepared at ca. 2.00 × 10^{-3} M. Metal ion solutions were prepared in water at 0.025−0.050 M from analytical grade nitrate salts of the metal ions and standardized by titration with Na_2H_2edta.[63] Carbonate-free solutions of the titrant KOH were prepared from a Merck ampule diluted 1 L of water (freshly boiled for about 2 h and allowed to cool under nitrogen). These solutions were standardized by application of Gran's method.[64] A 0.100 M standard solution of HNO_3 prepared from a commercial ampule was used for backtitrations. The [H$^+$] of the solutions was determined by measurement of the electromotive force of the cell, $E = E^{o\prime} + Q\log[H^+] + E_j$. The term pH is defined as −log [H$^+$]. $E^{o\prime}$ and Q were determined by titrating a solution of known hydrogen-ion concentration at the same ionic strength in the acid pH region. The liquid-junction potential, E_j, was found to be negligible under the experimental conditions used. The value of $K_w = [H^+][OH^-]$ was found to be equal to 10$^{-13.78}$ by titrating a solution of known hydrogen-ion concentration at the same ionic strength in the alkaline pH region, considering $E^{o\prime}$ and Q valid for the entire pH range.

Measurements were carried out with ca. 0.05 mmol of ligand in a total volume of ca. 30 mL, in the absence of metal ions and in the presence of each metal ion at 0.9 equiv ratio. A backtitration was always performed at the end of each direct titration in order to check if equilibrium was attained throughout the full pH range. Each titration curve typically consisted of 50−60 points at the 2.5−11.5 pH range, and a minimum of two replicate titrations were performed for each system.

Out-of-cell (batch) titrations were carried out for systems displaying very slow complexation kinetics, which happened for Cu^{2+} with H_2do2ph, and for Cu^{2+} and Zn^{2+} with H_2cb-do2ph. Each of these titrations consisted of a set of independent points at different pH values prepared in the same experimental conditions used for the conventional titrations, but at 1/10 of the total volume. The vials containing each point were tightly closed under nitrogen and kept at 298.2 K until equilibrium was reached, which was verified by pH measurement each week. A mother solution of the complex was prepared by addition of the ligand and metal ion in 1:0.9 ratio. For the complexes of both ligands the equilibrium was generally reached after 2−3 weeks.

NMR Titrations. For determination of all protonation constants from H_2do2ph and the last three protonation constants from H_2cb-do2ph, ^{1}H NMR spectra were recorded in D_2O solution at 298.2 K, ca. 40 points per titration. The ligand stock solutions were prepared at ca. 2 × 10^{-3} M without control of the ionic strength, and the titrant was a freshly prepared CO_2-free KOD solution. The titrations were performed directly in the NMR tube, and the titrant was added with a micropipet. The pH* was measured with an Orion Star A214 pH/ISE meter fitted with a Hamilton Spintrode PN23819703 combined microelectrode upon calibration with commercial buffers in aqueous solution (pH of 12.00, 8.00, and 4.00). The final pD was calculated according to the equation pD = pH* + (0.40 ± 0.02),[65] where pH* corresponds to the reading on the pH meter. The equilibrium constants determined in D_2O (K_D) were converted to H_2O (K_H) values using published equations.[66]

Thermodynamic Equilibrium Constants Determination. Data from potentiometric titrations were used to determine the protonation constants of H_2do2ph and H_2cb-do2ph, except the first one, and the stability constants with the different metal ions. ^{1}H NMR titrations were used to confirm the magnitude of all protonation constants from H_2do2ph and the last three protonation constants from H_2cb-do2ph. The overall equilibrium constants β_i^H and $\beta_{M_mH_hL_l}$ (being $\beta_{M_mH_hL_l} = [M_mH_hL_l]/[M]^m[H]^h[L]^l$ and $\beta_{MH-1L} = \beta_{ML(OH)} \times K_w$) were obtained by refinement of the potentiometric data with the HYPERQUAD program,[67] and of the ^{1}H NMR data by the HYPNMR program.[68] Differences, in log units, between the values of protonated (or hydrolyzed) and nonprotonated constants provide the stepwise (log K) constants (being $K_{M_mH_hL_l} = [M_mH_hL_l]/[M_mH_{h-1}L_l][H]$). The errors quoted are the standard deviations of the overall stability constants calculated by the program when all the experimental data. At least two titration curves for each system were fitted together. Species distribution diagrams were plotted from the calculated constants with the HYSS program.[69]

Kinetic Inertness of the Copper(II) and Gallium(III) Complexes. The acid-assisted dissociation of the copper(II) complexes of both ligands was studied in 1 M HCl aqueous solution under pseudo-first-order conditions at 298.2, 303.2, 310.2, 333.2, and 363.2 K. Dissociation experiments were performed by following the spectral

dx.doi.org/10.1021/ic403156h | Inorg. Chem. 2014, 53, 4371−4386

absorption band of the complexes at 645 nm for [Cu(do2ph)] and at 615 nm for [Cu(cb-do2ph)]. The concentration of the complexes in the experiments was at 3.9×10^{-3} and 1.8×10^{-3} M, respectively, without any control of the ionic strength. The base-assisted dissociation of the gallium(III) complex of H_2do2ph in aqueous solution was studied by ^{71}Ga NMR spectroscopy. Sample solutions were prepared at ca. 5 mM in preformed complex and 200 mM in potassium carbonate buffer (pH = 11.0), and sample spectra were taken at random times using an insert tube containing 5 mM $[Ga(H_2O)_6]^{3+}$ in 0.1 M HCl as internal reference. The increasing peak of the $[Ga(OH)_4]^-$ resonance resulting from complex dissociation was integrated relative to the invariable one from $[Ga(H_2O)_6]^{3+}$ of the reference, so as to follow the variation of complex concentration with time. All kinetic data were processed by exponential regression to calculate the half-lives from the fitting equations.

Electrochemical Studies. Cyclic voltammetry experiments used a BAS CV-50W voltammetric analyzer connected to BAS/Windows data acquisition software. Measurements were performed in a glass cell MF-1082 from BAS in a C-2 cell enclosed in a Faraday cage, at rt, under nitrogen. The reference electrode was Ag/AgCl (MF-2052 from BAS) filled with 3 M NaCl in water, standardized for the redox couple $Fe(CN)_6^{3-}/Fe(CN)_6^{4-}$. The auxiliary electrode was a 7.5 cm platinum wire (MW-1032 from BAS) with a gold-plated connector. The working electrode was a glassy carbon (MF-2012 from BAS).

Copper(II) complexes of H_2do2ph and H_2cb-do2ph (at pH 10.0 and pH 9.4, respectively) were prepared in aqueous solution at ca. 1 mM using NaOAc 0.10 M as the supporting electrolyte. The solutions were deaerated by a nitrogen stream prior to all measurements, and were kept under nitrogen during the measurements. Between each scan the working electrode was electrocleaned by multicycle scanning in the supporting electrolyte solution, polished on alumina 1 and 0.05 μm, cleaned with water, and sonicated before use, according to standard procedures.

■ ASSOCIATED CONTENT

Supporting Information

1D and 2D NMR spectra of the compounds H_2do2ph and H_2cb-do2ph and their precursors; ^{1}H NMR spectra of the zinc(II) complex of H_2do2ph; ^{1}H, ^{13}C, and 2D NMR spectra of the gallium(III) complex of H_2do2ph; variable temperature ^{1}H NMR spectra of the gallium(III) complex of H_2do2ph; ESI mass spectra of H_2do2ph and its copper(II) and gallium(III) complexes; ESI mass spectra of H_2cb-do2ph and its copper(II) complex; species distribution diagrams of both ligands, their zinc(II) complexes, and the calcium(II) complex of H_2do2ph; UV spectra of both ligands at different pH values; Arrhenius plots for the acid-assisted dissociation of complexes of copper(II) with both ligands; and voltammograms of both copper(II) complexes in aqueous solution. This material is available free of charge via the Internet at http://pubs.acs.org.

■ AUTHOR INFORMATION

Corresponding Author

*E-mail: delgado@itqb.unl.pt.

Notes

The authors declare no competing financial interest.

■ ACKNOWLEDGMENTS

The authors acknowledge Fundação para a Ciência e a Tecnologia (FCT), with coparticipation of the European Community funds FEDER, POCI, QREN, and COMPETE, for the financial support and the fellowship of J.M. under Project PTDC/QUI/67175/2006. The authors also acknowledge support by Fundação para a Ciência e a Tecnologia (RECI/BBB-BQB/0230/2012) for the NMR spectrometers as part of the National NMR Facility. M. C. Almeida from the ITQB Analytical Services Unit is acknowledged for providing elemental analysis and ESI-MS data. The authors also thank Pedro Lamosa for the help on some $[Ga(do2ph)]^+$ NMR experiments. C.V.E. thanks FCT for the grant (SFRH/BD/89501/2012). P.M. and L.M.P.L. acknowledge FCT also for the postdoctoral fellowships SFRH/BPD/79518/2011 and SFRH/BPD/73361/2010, respectively.

■ REFERENCES

(1) Price, E. W.; Orvig, C. *Chem. Soc. Rev.* **2014**, *43*, 260−290.
(2) Cutler, C. S.; Hennkens, H. M.; Sisay, N.; Huclier-Markai, S.; Jurisson, S. S. *Chem. Rev.* **2013**, *113*, 858−883.
(3) Wadas, T. J.; Wong, E. H.; Weisman, G. R.; Anderson, C. J. *Chem. Rev.* **2010**, *110*, 2858−2902.
(4) Shokeen, M.; Anderson, C. J. *Acc. Chem. Res.* **2009**, *42*, 832−841.
(5) Parker, D. *Chem. Soc. Rev.* **1990**, *19*, 271−291.
(6) Pandya, D. N.; Dale, A. V.; Kim, J. Y.; Lee, H.; Ha, Y. S.; Il An, G.; Yoo, J. *Bioconjugate Chem.* **2012**, *23*, 330−335.
(7) Odendaal, Y.; Fiamengo, A. L.; Ferdani, R.; Wadas, T. J.; Hill, D. C.; Peng, Y.; Heroux, K. J.; Golen, J. A.; Rheingold, A. L.; Anderson, C. J.; Weisman, G. R.; Wong, E. H. *Inorg. Chem.* **2011**, *50*, 3078−3086.
(8) Wadas, T. J.; Wong, E. H.; Weisman, G. R.; Anderson, C. J. *Curr. Pharm. Des* **2007**, *13*, 3−16.
(9) Woodin, K. S.; Heroux, K. J.; Boswell, C. A.; Wong, E. H.; Weisman, G. R.; Niu, W.; Tomellini, S. A.; Anderson, C. J.; Zakharov, L. N.; Rheingold, A. L. *Eur. J. Inorg. Chem.* **2005**, 4829−4833.
(10) Esteves, C. V.; Lamosa, P.; Delgado, R.; Costa, J.; Désogère, P.; Rousselin, Y.; Goze, C.; Denat, F. *Inorg. Chem.* **2013**, *52*, 5138−5153.
(11) Bernier, N.; Costa, J.; Delgado, R.; Félix, V.; Royal, G.; Tripier, R. *Dalton Trans.* **2011**, *40*, 4514−4526.
(12) Sun, X.; Wuest, M.; Weisman, G. R.; Wong, E. H.; Reed, D. P.; Boswell, C. A.; Motekaitis, R.; Martell, A. E.; Welch, M. J.; Anderson, J. *J. Med. Chem.* **2002**, *45*, 469−477.
(13) Ramogida, C. F.; Orvig, C. *Chem. Commun.* **2013**, *49*, 4720−4739.
(14) Delgado, R.; Félix, V.; Lima, L. M. P.; Price, D. W. *Dalton Trans.* **2007**, 2734−2745.
(15) Bandoli, G.; Dolmella, A.; Tisato, F.; Porchia, M.; Refosco, F. *Coord. Chem. Rev.* **2009**, *253*, 56−77.
(16) Fani, M.; André, J. P.; Maecke, H. R. *Contrast Media Mol. Imaging* **2008**, *3*, 53−63.
(17) Nayak, T. K.; Brechbiel, M. W. *Bioconjugate Chem.* **2009**, *20*, 825−841.
(18) Bhattacharyya, S.; Dixit, M. *Dalton Trans.* **2011**, *40*, 6112−6128.
(19) Dapporto, P.; Fusi, V.; Micheloni, M.; Palma, P.; Paoli, P.; Pontellini, R. *Inorg. Chim. Acta* **1998**, *275*−*276*, 168−174.
(20) Esteves, C. V.; Lima, L. M. P.; Mateus, P.; Delgado, R.; Brandão, P.; Félix, V. *Dalton Trans.* **2013**, *42*, 6149−6160.
(21) Rohovec, J.; Gyepes, R.; Císařová, I.; Rudovský, J.; Lukeš, I. *Tetrahedron Lett.* **2000**, *41*, 1249−1253.
(22) Weisman, G. R.; Wong, E. H.; Hill, D. C.; Rogers, M. E.; Reed, D. P.; Calabrese, C. *Chem. Commun.* **1996**, 947−948.
(23) Hervé, G.; Bernard, H.; Le Bris, N.; Le Baccon, M.; Yaouanc, J.-J.; Handel, H. *Tetrahedron Lett.* **1999**, *40*, 2517−2520.
(24) Sanders, R. W.; Gacek, M.; Undheim, K. *Acta Chim. Scand.* **1998**, *52*, 1402−1404.
(25) Baker, W. C.; Choi, V.; Hill, D. C.; Thompson, J. L.; Petillo, P. A. *J. Org. Chem.* **1999**, *64*, 2683−2689.
(26) De León-Rodríguez, L. M.; Kovacs, Z.; Esqueda-Oliva, A. C.; Miranda-Olvera, A. D. *Tetrahedron Lett.* **2006**, *47*, 6937−6940.
(27) Dale, J. *Acta Chem. Scand.* **1973**, *27*, 1115−1129.
(28) Addison, A. W.; Rao, T. N.; Reedijk, J.; van Rijn, J.; Verschoor, G. C. *J. Chem. Soc., Dalton Trans.* **1984**, 1349−1356.
(29) Heppeler, A.; Froidevaux, S.; Mäcke, H. R.; Jerman, E.; Béhé, M.; Powell, P.; Hennig, M. *Chem.—Eur. J.* **1999**, *5*, 1974−1981.
(30) Viola, N. A.; Rarig, R. S., Jr.; Ouellette, W.; Doyle, R. P. *Polyhedron* **2006**, *25*, 3457−3462.
(31) Yang, C.-T.; Li, Y.; Liu, S. *Inorg. Chem.* **2007**, *46*, 8988−8997.

(32) Heppeler, A.; André, J. P.; Buschmann, I.; Wang, X.; Reubi, J.-C.; Hennig, M.; Kaden, T. A.; Maecke, H. R. *Chem.—Eur. J.* **2008**, *14*, 3026−3034.
(33) Kubíček, V.; Havlíčková, J.; Kotek, J.; Tircsó, G.; Hermann, P.; Tóth, É.; Lukeš, I. *Inorg. Chem.* **2010**, *49*, 10960−10969.
(34) Bosnich, B.; Poon, C. K.; Tobe, M. L. *Inorg. Chem.* **1965**, *4*, 1102−1108.
(35) Niu, W.; Wong, E. H.; Weisman, G. R.; Peng, Y.; Anderson, C. J.; Zakharov, L. N.; Golen, J. A.; Rheingold, A. L. *Eur. J. Inorg. Chem.* **2004**, 3310−3315.
(36) Weeks, J. M.; Taylor, M. R.; Wainwright, K. P. *J. Chem. Soc., Dalton Trans.* **1997**, 317−322.
(37) Chaves, S.; Delgado, R.; Fraústo da Silva, J. J. R. *Talanta* **1992**, *39*, 249−254.
(38) Delgado, R.; Fraústo da Silva, J. J. R. *Talanta* **1982**, *29*, 815−822.
(39) Pettit, L. D.; Powell, H. K. J. *IUPAC Stability Constants Database*; Academic Software: Timble, U.K., 2003.
(40) Clarke, E. T.; Martell, A. E. *Inorg. Chim. Acta* **1991**, *190*, 37−46.
(41) Motekaitis, R. J.; Martell, A. E. *Inorg. Chem.* **1980**, *19*, 1646−1651.
(42) Delgado, R.; Sun, Y.; Motekaitis, R. J.; Martell, A. E. *Inorg. Chem.* **1993**, *32*, 3320−3326.
(43) Clarke, E. T.; Martell, A. E. *Inorg. Chim. Acta* **1991**, *181*, 273−280.
(44) Šimeček, J.; Schulz, M.; Notni, J.; Plutnar, J.; Kubíček, V.; Havlíčková, J.; Hermann, P. *Inorg. Chem.* **2012**, *51*, 577−590.
(45) SpinCount is a Windows software package that allows quantitative interpretation and simulation of EPR spectra, created by Professor M. P. Hendrich at Carnegie Mellon University. SpinCount is available at http://www.chem.cmu.edu/groups/hendrich/.
(46) Hathaway, B. J.; Tomlinson, A. A. G. *Coord. Chem. Rev.* **1970**, *5*, 1−43.
(47) Hathaway, B. J.; Billing, D. E. *Coord. Chem. Rev.* **1970**, *5*, 143−207.
(48) Lever, A. B. P. *Inorganic Electronic Spectroscopy*, 2nd ed.; Elsevier: Amsterdam, 1984; pp 554−572.
(49) Hathaway, B. J. *Coord. Chem. Rev.* **1983**, *52*, 87−169.
(50) Valko, M.; Morris, H.; Mazúr, M.; Telser, J.; McInnes, E. J. L.; Mabbs, F. E. *J. Phys. Chem. B* **1999**, *103*, 5591−5597.
(51) Billing, D. E.; Hathaway, B. J. *J. Chem. Soc. A* **1969**, 1516−1519.
(52) Lommens, P.; Feys, J.; Vrielinck, H.; De Buysser, K.; Herman, G.; Callens, F.; Van Driessche, I. *Dalton Trans.* **2012**, *41*, 3574−3582.
(53) Rakhit, G.; Sarkar, B. *J. Inorg. Biochem.* **1981**, *15*, 233−241.
(54) Peisach, J.; Blumberg, W. E. *Arch. Biochem. Biophys.* **1974**, *165*, 691−708.
(55) Styka, M. C.; Smierciak, R. C.; Blinn, E. L.; DeSimone, R. E.; Passariello, J. V. *Inorg. Chem.* **1978**, *17*, 82−86.
(56) Notni, J.; Hermann, P.; Havlíčková, J.; Kotek, J.; Kubíček, V.; Plutnar, J.; Loktionova, N.; Riss, P.; Rösch, F.; Lukeš, I. *Chem.—Eur. J.* **2010**, *16*, 7174−7185.
(57) Bell, C. A.; Bernhardt, P. V.; Gahan, L. R.; Martínez, M.; Monteiro, M. J.; Rodríguez, C.; Sharrad, C. A. *Chem.—Eur. J.* **2010**, *16*, 3166−3175.
(58) Hubin, T. J.; Alcock, N. W.; Morton, M. D.; Busch, D. H. *Inorg. Chim. Acta* **2003**, *348*, 33−40.
(59) Karlin, K. D.; Cohen, B. I.; Hayes, J. C.; Farooq, A.; Zubieta, J. *Inorg. Chem.* **1987**, *26*, 147−153.
(60) Le Baccon, M.; Chuburu, F.; Toupet, L.; Händel, H.; Soibinet, M.; Déchamps-Olivier, I.; Barbier, J.-P.; Aplincourt, M. *New J. Chem.* **2001**, *25*, 1168−1174.
(61) Sheldrick, G. M. *Acta Crystallogr.* **2008**, *A64*, 112−122.
(62) Farrugia, L. J. *J. Appl. Crystallogr.* **1999**, *32*, 837−83.
(63) Schwarzenbach, G.; Flaschka, W. *Complexometric Titrations*; Methuen & Co: London, 1969.
(64) Rossotti, F. J. C.; Rossotti, H. *J. Chem. Educ.* **1965**, *42*, 375−378.
(65) Delgado, R.; Fraústo da Silva, J. J. R.; Amorim, M. T. S.; Cabral, M. F.; Chaves, S.; Costa, J. *Anal. Chim. Acta* **1991**, *245*, 271−282.
(66) Krężel, A.; Bal, W. *J. Inorg. Biochem.* **2004**, *98*, 161−166.
(67) Gans, P.; Sabatini, A.; Vacca, A. *Talanta* **1996**, *43*, 1739−1753.
(68) Frassineti, C.; Ghelli, S.; Gans, P.; Sabatini, A.; Moruzzi, M. S.; Vacca, A. *Anal. Biochem.* **1995**, *231*, 374−382.
(69) Alderighi, L.; Gans, P.; Ienco, A.; Peters, D.; Sabatini, A.; Vacca, A. *Coord. Chem. Rev.* **1999**, *184*, 311−318.

NOTE ADDED AFTER ASAP PUBLICATION

This paper was published on the Web on April 22, 2014, with a minor text error. The corrected version was reposted on April 23, 2014.